Chemical Geology 608 (2022) 121024

Contents lists available at ScienceDirect

Chemical Geology

journal homepage: www.elsevier.com/locate/chemgeo

Capturing the short-term variability of carbon dioxide emissions from sedimentary rock weathering in a remote mountainous catchment, New Zealand

Tobias Roylands [a,*], Robert G. Hilton [a,b], Mark H. Garnett [c], Guillaume Soulet [a,d], Josephine-Anne Newton [c], Joanne L. Peterkin [e], Peter Hancock [f]

[a] Department of Geography, Durham University, South Road, Durham DH1 3LE, United Kingdom
[b] Department of Earth Sciences, University of Oxford, South Parks Road, Oxford OX1 3AN, United Kingdom
[c] NEIF Radiocarbon Laboratory, Rankine Avenue, East Kilbride, Glasgow G75 0QF, United Kingdom
[d] Geo-Ocean, Brest University, CNRS, Ifremer, F-29280 Plouzané, France
[e] Department of Earth Sciences, Durham University, South Road, Durham DH1 3LE, United Kingdom
[f] Gisborne District Council, 15 Fitzherbert Street, PO Box 747, Gisborne 4010, New Zealand

ARTICLE INFO

Editor: Christian France-Lanord

Keywords:
Oxidative weathering
Petrogenic organic carbon
Carbon dioxide
Carbon isotopes
Microbial respiration
Silicate weathering

ABSTRACT

Weathering of organic carbon contained in sedimentary rocks (petrogenic OC, OC_{petro}) is an important control on the concentrations of carbon dioxide (CO_2) and oxygen in the atmosphere. Of particular significance are steep mountainous catchments, where high rates of physical erosion introduce OC_{petro} to the surface, where oxygen in air and water can help drive oxidative weathering reactions, yet measurements of CO_2 emissions from OC_{petro} oxidation are still scarce. Here, we use in situ gas accumulation chambers and show that CO_2 fluxes, and their environmental controls, can be determined during a stand-alone, short-term (8 days) field campaign, applied to a remote setting. In the rapidly eroding Waiapu River catchment, New Zealand, dominated by mudstones, we measured high rates of CO_2 release (222–1590 mgC m^{-2} d^{-1}) in five accumulation chambers in the near-surface of naturally fractured and bedded rock outcrops. The corresponding CO_2 concentrations are very high (pCO_2 ~4700–27,100 ppmv), and such values could influence acid-hydrolysis reactions during chemical weathering of co-occurring silicate minerals. The CO_2 is radiocarbon depleted (fraction modern, $F^{14}C$ = 0.0122–0.0547), confirming it is petrogenic in origin. Stable carbon isotopes suggest a source from OC_{petro}, but $\delta^{13}C$ values of the CO_2 are lower by ~3.5–3.7 ± 0.1 ‰ from those of OC_{petro} (−25.9 ± 0.1 ‰), consistent with isotope fractionation associated with microbial respiration of OC_{petro}. Over 6 days of measurement, we find that CO_2 fluxes respond quickly to changes in temperature and humidity, indicating an environmental regulation that is captured by our short-term installation. The approaches applied here mean that future research can now seek to constrain the climatic, lithological and biological controls on OC_{petro} oxidation across regional to global scales.

1. Introduction

Earth's sedimentary rocks contain around 130,000 times more carbon (~75×10^9 Mt) than the pre-industrial atmosphere, of which ~80% are present in the form of inorganic minerals (carbonates) and ~20% organic carbon (petrogenic OC, OC_{petro}), respectively (Petsch, 2014). Over geological timescales, small changes in the balance between the deposition of sedimentary carbon and its weathering on land can alter the concentration of carbon dioxide (CO_2) and oxygen (O_2) in the atmosphere (Berner, 1999; Sundquist and Visser, 2003). These govern the planet's habitability, climate and composition of the oceans and atmosphere (Bergman et al., 2004; Berner, 2004).

Steep mountainous areas are responsible for more than half of the planet's denudation, with rapid rates of physical erosion and chemical weathering (Larsen et al., 2014). As such, these locations are important for the global exchange of carbon between rocks and the atmosphere (Hilton and West, 2020). In terms of silicate weathering by carbonic acid, which acts as a carbon sink when the weathering products are coupled to the precipitation of new carbonate minerals (Berner, 1999; Chamberlin, 1899; Walker et al., 1981), erosive settings can have high

* Corresponding author.
E-mail address: tobias.roylands@outlook.de (T. Roylands).

https://doi.org/10.1016/j.chemgeo.2022.121024
Received 19 October 2021; Received in revised form 29 June 2022; Accepted 18 July 2022
Available online 21 July 2022

weathering fluxes (Larsen et al., 2014; Milliman and Syvitski, 1992), but more importantly are where the climate-sensitivity of silicate weathering is most pronounced (Maher and Chamberlain, 2014; West et al., 2005). They are also places where the erosion of organic carbon from the biosphere can be rapid (Galy et al., 2015; Hilton, 2017), which, when coupled to burial, acts as a CO_2 sink (Berner, 1999). However, it is increasingly recognized that, depending on the lithological composition, oxidative weathering reactions can lead to a CO_2 release (Calmels et al., 2007; Hilton et al., 2014; Petsch, 2014; Torres et al., 2014) that can dominate the net rock-atmosphere exchange of CO_2 during weathering and erosion (Hilton and West, 2020).

During chemical weathering, the oxidation of OC_{petro} produces CO_2 and consumes O_2, so-called georespiration (Berner, 1999; Keller and Bacon, 1998; Petsch, 2014):

$$CH_2O + O_2 \rightarrow CO_2 + H_2O. \quad (1)$$

Another source of CO_2 during chemical weathering can be via the oxidation of sulfide minerals (Calmels et al., 2007; Li et al., 2008; Torres et al., 2014). In this process, sulfuric acid released from the oxidation of sulfides (e.g., pyrite) can lead to in situ emission of CO_2 by dissolving neighboring carbonates:

$$CaCO_3 + H_2SO_4 \rightarrow CO_2 + H_2O + Ca^{2+} + SO_4^{2-}. \quad (2)$$

Alternatively, the CO_2 can be released elsewhere (e.g., by impacting the carbonate system of stream and river water) and when considering the timescale of carbonate precipitation in the oceans ($\sim 10^6$ yr) (Berner, 2004). This can be described by the equations

$$2CaCO_3 + H_2SO_4 \rightarrow 2Ca^{2+} + SO_4^{2-} + 2HCO_3^- \quad (3)$$

and

$$Ca^{2+} + 2HCO_3^- \rightarrow CaCO_3 + CO_2 + H_2O. \quad (4)$$

The global CO_2 fluxes derived from oxidative weathering are known well enough to be recognized as important players in the geological carbon cycle (Hilton and West, 2020), with estimates of OC_{petro} oxidation (40–100 MtC yr^{-1}) (Petsch, 2014) and sulfide oxidation (31–36 MtC yr^{-1}) (Berner and Berner, 2012; Burke et al., 2018) comparable in size to the CO_2 drawdown by silicate weathering (90–140 MtC yr^{-1}) (Gaillardet et al., 1999; Moon et al., 2014). Previous research has suggested that oxidative weathering is controlled by various environmental factors, such as temperature, oxygen availability, hydrology, erosion rates and lithology (Bolton et al., 2006; Chang and Berner, 1999; Hemingway et al., 2019; Hilton et al., 2014; Soulet et al., 2021). However, they are not well constrained compared to the analogous controls of silicate weathering (Maher and Chamberlain, 2014; Walker et al., 1981; West et al., 2005). In addition, rock weathering can be affected by microorganisms, which can form biofilms around minerals contributing to and accelerating their breakdown (Ehrlich et al., 2015). This seems to be true for oxidative weathering of sedimentary organic matter, with a growing body of work highlighting the potential for microbes to thrive on and incorporate OC_{petro}, with evidence from weathering profiles and laboratory incubations (Bardgett et al., 2007; Berlendis et al., 2014; Matlakowska and Sklodowska, 2011; Petsch et al., 2001; Seifert et al., 2013, 2011). Despite the potential of microorganisms to enzymatically influence the oxidation of OC_{petro}, it is unknown how the net weathering rate and CO_2 release are affected in natural environments (Hemingway et al., 2018; Stasiuk et al., 2017; Włodarczyk et al., 2018).

Research addressing the fate of sedimentary organic carbon undergoing weathering has so far focused mostly on indirect approaches, using river data that describe the export of OC_{petro} from a catchment, which can be used to estimate the amount of organic matter that escapes oxidation (Bouchez et al., 2010; Hilton et al., 2011), or trace element proxies have been applied at the river catchment scale (e.g., Dalai et al., 2002; Hilton et al., 2014). However, this scale of investigation cannot directly track the reactions in situ, thus obscuring how biogeochemical processes and environmental variables, such as temperature, control oxidative weathering processes. In order to better understand regional and global patterns of oxidative weathering and their environmental controls, we require measurements from a variety of settings (Longbottom and Hockaday, 2019). In situ measurements of CO_2 emissions that identify a rock-derived component have only been reported from two sites (Keller and Bacon, 1998; Soulet et al., 2021, 2018). Following the method described by Soulet et al. (2018), rock-derived CO_2 can be differentiated from modern sources (such as soils or the atmosphere) using radiocarbon analyses, whereas radiocarbon-free contributions from OC_{petro} and sulfide oxidation coupled to carbonate dissolution can be partitioned using the stable carbon isotope compositions.

Here we explore whether CO_2 emissions from oxidative weathering and their environmental controls can be captured using stand-alone, short-term field campaigns. We do this by installing in situ weathering chambers in the remote and rapidly eroding Waiapu catchment, New Zealand. In this area, OC_{petro} bearing rocks are widespread (Leithold et al., 2006; Thompson, 2009) and the physical erosion rates are well described (Hicks et al., 2004; Marden et al., 2012; Parkner et al., 2006), supplying OC_{petro} to the weathering zone. We measure CO_2 fluxes that appear rapid when compared to other weathering fluxes (e.g., silicate weathering) and approach values of soil respiration. In contrast to the only other study of this type (Soulet et al., 2021, 2018), we find that the CO_2 fluxes are dominated by OC_{petro} oxidation, with no evidence for carbonate-derived CO_2. The OC_{petro} weathering fluxes vary over the installation, and we explore how this variability can be explained by changes in precipitation/hydrology and temperature. In addition, the potential microbial impact on the oxidation of OC_{petro} and the carbon isotope composition of emitted CO_2 is discussed. Finally, we examine the wider implications for the understanding of Earth's geological carbon cycle including the weathering of silicate minerals in sedimentary rocks.

2. Material and methods

2.1. Study site

The study site is located within the Waiapu River catchment, North Island, New Zealand (Fig. 1), situated on the active margin of the converging Pacific and Australian plates and part of the Hikurangi Accretionary Prism (Shulmeister, 2017). This setting is characterized by tectonic uplift of ~4 mm yr^{-1} in the Late Quaternary (Litchfield and Berryman, 2006) and the tectonic setting results in active fault systems and occasional methane gas and oil seeps in the region (Reyes et al., 2010). Generally, the lithology of the Waiapu catchment is dominated by intensely deformed Cretaceous and Tertiary sedimentary rocks (Mazengarb and Speden, 2000).

In the Northeast of New Zealand, several stations for environmental monitoring are run by the Gisborne District Council including data records on air temperature, rainfall and river flow for the Waiapu catchment (Fig. 1). The mean annual rainfall is ~2 m yr^{-1} in a temperate maritime climate where storms arrive from the tropics around once to twice a year (Chappell, 2016). The combination of these intense rainfall events with easily erodible rocks and high rates of tectonic uplift result in high erosion rates, which have been further increased due to widespread deforestation in the late nineteenth and early twentieth century (Hicks et al., 2004; Marden et al., 2012; Parkner et al., 2006). In the Waiapu River basin, a fifth of the terrain is susceptible to gully erosion and sediment is generated primarily by mass movement processes following oversteepening of gully sidewalls by channel incision, leading to a very high suspended sediment yield of 17,800 t km^{-2} yr^{-1} (Betts et al., 2003; Hicks et al., 2004). Taking the bedrock density into account, an average erosion rate of ~7 mm yr^{-1} can be estimated for the Waiapu catchment, indicating short residence times of the abundant exposed bedrock and regolith (Fig. 1) (Leithold et al., 2006). Chemical weathering fluxes are constrained by long-term discharge data and spot river samples (Lyons et al., 2005), and they are very high (400 t km^{-2} yr^{-1}),

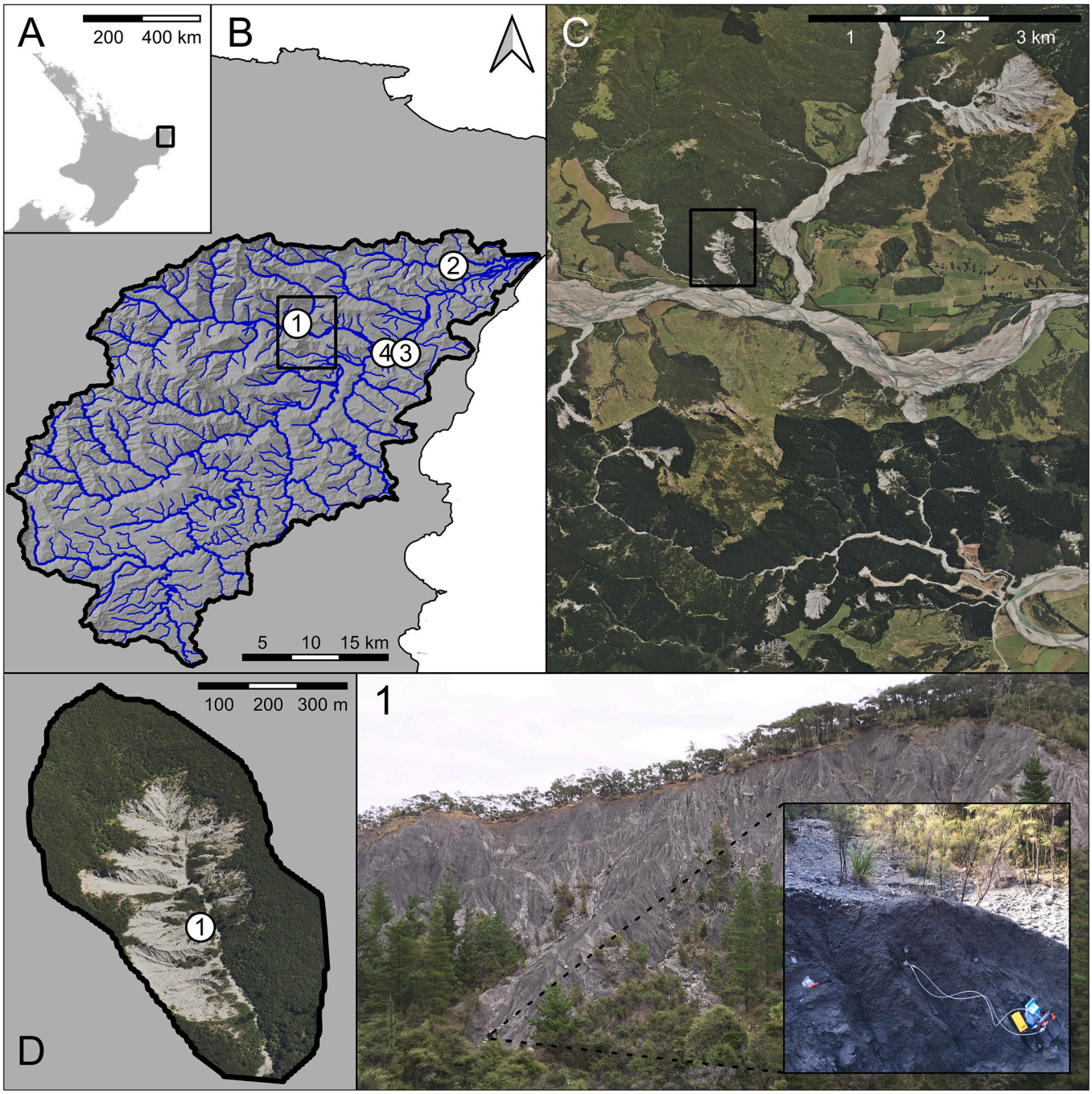

Fig. 1. Map and imagery of the study area. A) Location of the Waiapu catchment in the Northeast of New Zealand. B) Location of the study site (1) and environmental monitoring stations in the Waiapu catchment: Poroporo Fire Station for air temperatures (2), Ruatoria Telemetry Station for rainfall data (3), and Rotokautuku Bridge for Waiapu River flow (4). C) Exposed rocks and regolith occur frequently in the surrounding of the study area. D) Location of the experimental setup (1) in a rapidly eroding gully complex. Panels A) to D) are based on data and satellite imagery provided from the Land Information New Zealand (LINZ) Data Service under the Creative Commons Attribution 4.0 International License.

with silicate weathering (1.9×10^5 mol km^{-2} yr^{-1}, total cation yield from silicate minerals) slightly dominating over carbonate weathering (1.2×10^5 mol km^{-2} yr^{-1}, Ca^{2+} yield from carbonate minerals).

Our site is located in one of the large gully complexes (0.37 km^2) that drains into the Tapuaeroa River (Fig. 1). It is underlain by Early Cretaceous mudstones of the Mokoiwi Formation (Ruatoria Group) and part of the Miocene East Coast Allochthon (Mazengarb and Speden, 2000). No gas or oil seep occurs in close proximity to the study site (Francis et al., 1991; Reyes et al., 2010; Scadden et al., 2016). Measurements of rocks from this region (Thompson, 2009) and the stable carbon isotope composition and radiocarbon activity of suspended sediments in the Waiapu River show OC_{petro} is widespread in the catchment (Leithold et al., 2006), with a concentration of ~0.4 wt% to 0.5 wt% in river sediments (Hilton, 2017).

2.2. CO_2 measurements

2.2.1. In situ weathering chambers

We installed gas accumulation chambers directly into rock outcrops undergoing weathering (Fig. 1) following the design established by

Table 1
Properties of gas accumulation chambers drilled into weathering sedimentary rocks in the Waiapu catchment, New Zealand (37.85986° S, 178.19028° E).

Chamber	Elevation above riverbed (m)	Installation date	Depth (cm)	Volume (cm^3)	Area of exchange with surrounding rock (cm^2)
H2	4.5	28/04/2018	42	227	334
H3	1.8	28/04/2018	43	229	336
H4	1.5	28/04/2018	44	237	344
H5	2.1	29/04/2018	48	269	361
H7	3.2	29/04/2018	12	64	79

Soulet et al. (2018). In summary, weathering chambers were drilled horizontally into the exposed rock face which was cleared of loose material beforehand. Their elongated cylinder-like shape ensures a large ratio of surface to volume that benefits CO_2 flux measurements and allows gases to be trapped for isotope analysis (Table 1). In order to install the chambers, we used a hand auger with a diameter of 2.6 cm. Then, a small PVC tube is inserted in the entrance of each chamber and closed with a rubber stopper holding two glass tubes fitted with Tygon® tubing, which allows either connection to a gas-sampling system or closure with WeLock® clips to isolate the chamber from the atmosphere. In addition, the intersection of the PVC tube and the surrounding rock is sealed with silicone sealant (Selleys Wet Area Silicone). In this design, the gas exchange between the chamber headspace and the rock pore space happens over the surface of the inner wall of the chamber (Soulet et al., 2018).

We installed seven chambers which were distributed evenly over a transect of ~10 m length in a small gully that was free of vegetation or soil (Fig. 1). A thermocouple meter (Digi-Sense), which was externally calibrated in the range of 5–25 °C, was placed inside one of the chambers to measure the internal temperature. Another chamber was installed as a back-up in case one was lost, for example, in the event of structural collapse. Four of the chambers had similar depths, but H7 was notably shorter (Table 1), which reflected a refusal depth of the hand drill. The chamber array started with H4 at 1.5 m elevation above the riverbed in which the gully drained, followed by H3, H5, H7, and H2 at 4.5 m elevation at the top of the transect, respectively (Table 1). The elevation was estimated to the nearest 1 m with a digital elevation model (8 m spatial resolution; Land Information New Zealand (LINZ) Data Service under the Creative Commons Attribution 4.0 International License), verified with GPS-derived altitude measurements, and estimated to the nearest 10 cm with scaled imagery taken in the field.

In addition, we collected rock powder from the drilling of the chambers and stored it in pre-combusted glass vials (4 h at 450 °C) at 4 °C (apart from transport) until freeze-drying.

2.2.2. Rock pCO_2 measurements

The concentrations of CO_2 in the chambers (pCO_2) were measured using an infra-red gas analyzer (EGM 5 Portable CO_2 Gas Analyzer, PP Systems), which is equipped with an internal pump and calibrated to a pCO_2 in the range of 0 ppmv to 30,000 ppmv, connected to a closed-loop CO_2 sampling system incorporating a CO_2 scrub (soda lime) and a water trap (magnesium perchlorate) as described by Hardie et al. (2005). Before measuring the CO_2 flux in a chamber, the ambient pCO_2 was determined by connecting the purged, CO_2-free sampling system to a chamber that was left closed overnight so that the CO_2 concentration in the surrounding rock pores and the chamber equilibrated. After a short equilibration, the rock pCO_2 can be calculated from the measured CO_2 concentration in the combined air volume of the chamber and the sampling system by accounting for the dilution introduced from the CO_2-free air that was originally contained within the sampling system (Soulet et al., 2018).

2.2.3. CO_2 flux measurements

Flux measurements of CO_2 from in situ weathering chambers have been described in detail previously (Soulet et al., 2018). In summary, the accumulation of CO_2 can be recorded over time after lowering the pCO_2 to a near-atmospheric value by the CO_2 scrub or a zeolite sieve (Section 2.2.4) mounted in parallel to the CO_2 monitoring line. One flux measurement consists of a series of repeatedly monitored CO_2 accumulations over ~6 min that are separated by short periods where the CO_2 is removed from the chamber to near-atmospheric values. The rate of CO_2 accumulation is then calculated by fitting an exponential model to the recorded pCO_2 change (Pirk et al., 2016), which considers the diffusivity of carbon from the rock to the chamber and the chamber leakiness (Soulet et al., 2018). The first three repeats are not used in the calculation of the flux, but instead to purge the CO_2 in the rock pores surrounding the chamber. A further three repeats are used to determine an average rate of CO_2 accumulation and its standard deviation. This flux is reported as the CO_2 accumulation rate normalized to the surface area of exchange with the surrounding rock to account for differences in the depth of the chambers that are related to differences in volume and surface area (Table 1).

2.2.4. CO_2 sampling and isotopic analyses

The CO_2 accumulations of a flux measurement can be sampled by circulating the chamber air through a zeolite molecular sieve sampling cartridge mounted in parallel to the CO_2 monitoring line (Hardie et al., 2005). In the chambers, CO_2 was sampled between day 5 (02/05/2018) and day 8 (05/05/2018) of the trip, and a total of 10 samples was collected. To yield a sufficient amount of CO_2 for isotopic analyses, a greater number of repeats was sampled for some measurements with lower fluxes. The volume of carbon loaded onto the sieves was quantified by adding up the pCO_2 maxima of the repeated accumulations of a flux measurement minus the near-atmospheric value (lower boundary of an accumulation) while accounting for the combined volume of the chamber and the sampling system.

The gas trapped onto the zeolite sieves was recovered in the laboratory by heating to 425 °C, while purging with high-purity nitrogen gas. The CO_2 was purified cryogenically under vacuum and its volume quantified (Garnett et al., 2019; Garnett and Murray, 2013). All volumes of CO_2 are normalized to 0 °C and 1013 mbar. The stable carbon isotope composition of the CO_2 was measured using Isotope Ratio Mass Spectrometry (IRMS; Thermo Fisher Delta V). The results are reported in standard delta (δ) notation in per mil (‰) relative to Vienna Pee Dee Belemnite (VPDB) standard. To determine the radiocarbon activity of CO_2, aliquots were graphitized by iron/zinc reduction and measured with Accelerator Mass Spectrometry at the Scottish Universities Environmental Research Centre (SUERC). Radiocarbon measurements were corrected for isotopic fractionation using the sample-specific $\delta^{13}C$ value and reported in the form of the fraction modern (i.e., in the $F^{14}C$ notation) (Reimer et al., 2004; Stuiver and Polach, 1977).

In addition, an atmospheric CO_2 sample was collected by circulating the atmosphere sampled at ~3 m above ground through a zeolite molecular sieve using the CO_2 sampling system and analyzed for its stable carbon isotope composition as described above.

2.3. Bulk geochemistry

The rock powder collected during the drilling of the accumulation chambers was analyzed for its bulk geochemical composition. After freeze-drying, it was ground and homogenized using a pestle and mortar. The stable carbon isotope composition of organic carbon and its

content were obtained using an Elemental Analyzer (Costech) coupled to an IRMS (Thermo Fisher Delta V Advantage) after inorganic carbon removal from the samples with aqueous HCl (4 mol L^{-1}). In summary, a known sample mass was weighed into pre-combusted silver capsules (combusted at 450 °C within a week of analysis) loaded into a Teflon tray, with acid added to each capsule and then placed in the oven at 80 °C until the liquid was evaporated (~2 h), and the acid step and drying repeated twice. Capsules were folded closed prior to analysis. The stable carbon isotope composition of inorganic carbon and its content were measured with a carbonate dissolution device (Thermo Scientific Gas Bench II) coupled to an IRMS (Thermo Scientific MAT 253). Furthermore, total sulfur measurements were performed with an Elemental Analyzer (Costech) coupled to an IRMS (Thermo Fisher Delta V Plus). Both stable carbon isotope compositions are reported in standard delta (δ) notation in per mil (‰) relative to Vienna Pee Dee Belemnite (VPDB) standard, whereas carbon and sulfur contents are reported in % weight.

Because the studied rocks are of Cretaceous origin, they should not contain any radiocarbon. We assume that their $F^{14}C$ values are zero when studying the carbon isotope mass balance in the weathering zone (Eq. (5)) (Soulet et al., 2018).

3. Results

3.1. Bulk geochemistry

The rocks of the Mokoiwi Formation are characterized by an average organic carbon concentration of 0.76 ± 0.23 wt% (± standard deviation, unless otherwise stated), with a $\delta^{13}C$ of −25.9 ± 0.1 ‰. In contrast, for most of the rock samples, the inorganic carbon content was below the detection threshold (0.1 wt%). For the remaining samples, they had inorganic carbon concentrations of 0.17 ± 0.06 wt% with a $\delta^{13}C$ of −10.7 ± 0.1 ‰. This $\delta^{13}C$ value is significantly more negative than typical $\delta^{13}C$ values from Early Cretaceous marine carbonates ranging between ~0 ‰ and + 5 ‰ (Erba, 2004; Gröcke et al., 2003; Weissert et al., 1998). This discrepancy could be the result of diagenesis and tectonic deformation of carbonate concretions, which are widespread in several outcropping lithologies in the Waiapu catchment (Mazengarb and Speden, 2000), and which occur with a wide range of $\delta^{13}C$ values between −50 ‰ and + 15 ‰ in Cretaceous and Cenozoic rocks in New Zealand (Nelson and Smith, 1996; Pearson and Nelson, 2005). Furthermore, total sulfur measurements revealed a content of 0.33 ± 0.04 wt%.

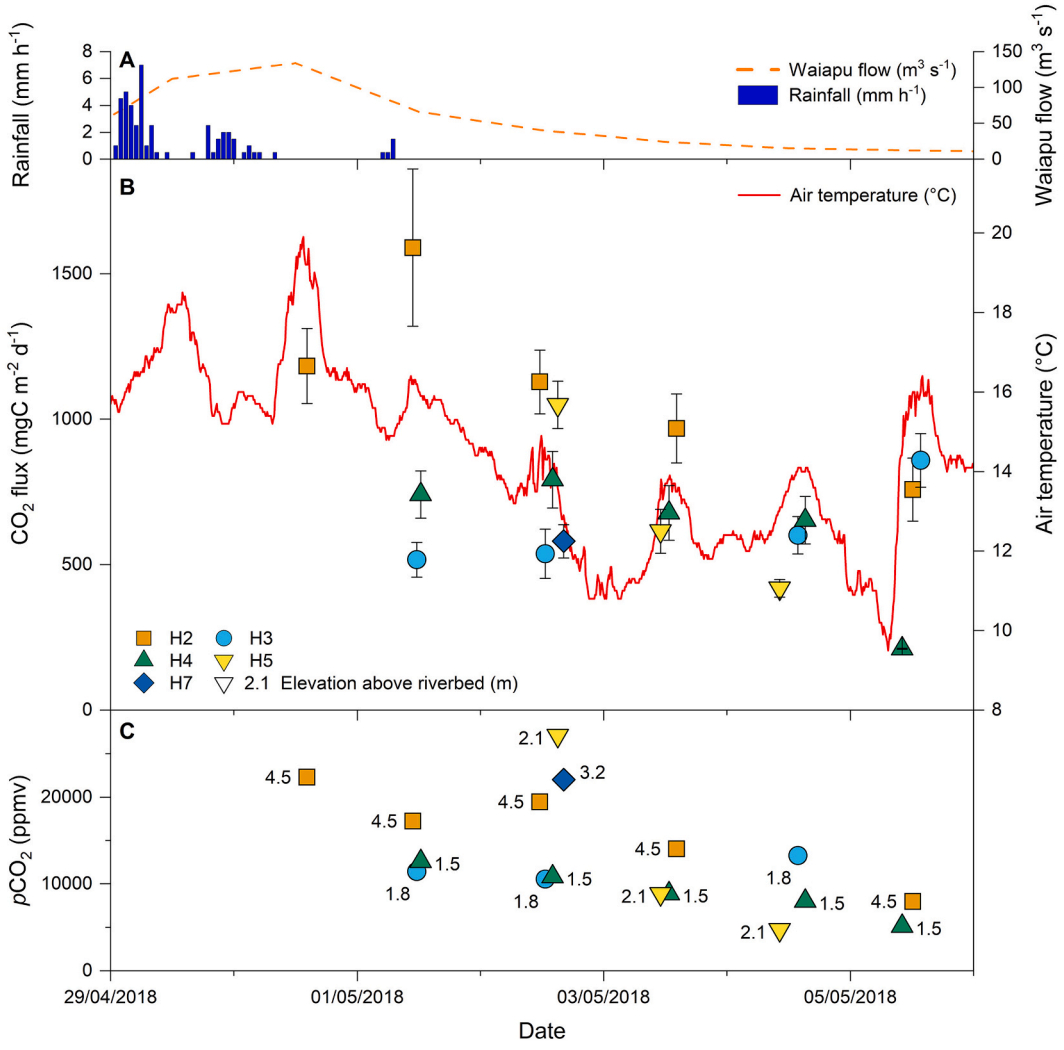

Fig. 2. Time series of carbon dioxide fluxes and partial pressures alongside environmental variables. A) Rainfall (mm h^{-1}) and flow of the Waiapu River (m^3 s^{-1}). B) Fluxes [CO_2] (mgC m^{-2} d^{-1}) with standard deviation from five in situ weathering chambers alongside air temperature at the Poroporo Fire Station (°C). C) Partial pressures [pCO_2] (ppmv) measured prior to each flux measurement. The elevation of the chambers above the riverbed (m) is denoted next to each partial pressure symbol.

3.2. Environmental variables

The start of the field trip coincided with a storm event in the Waiapu catchment, which delivered ~45 mm rainfall within 3 days, and resulted in an increase in the water discharge of the Waiapu River and its tributaries (Fig. 2A). This peaked on 30/04/2018. The chambers were installed between 28/04/2018 and 29/04/2018 (Table 1). In the following days, no significant precipitation occurred and the bare surface of the studied mudstones dried visibly. Over the 6 days of CO_2 measurements and the 2 days before, significant changes in air temperatures were recorded ranging from 9.5 °C to 19.9 °C at the Poroporo Fire station (~18 km from the site at ~164 m elevation) (Fig. 2B). The temperature record at Poroporo Fire station closely mirrors that measured in the rock face (dummy accumulation chamber at ~160 m elevation). Due to the short and incomplete character of the latter, this study benefits from including the more detailed air temperature record. The agreement between the datasets is best when considering a lag of around 2 h from the Poroporo Fire station to the rock chamber (Fig. 3).

3.3. CO_2 fluxes

Over the sampling period, the measured CO_2 fluxes varied between the gas accumulation chambers, and over time at each single chamber (Fig. 2-B). Overall, the CO_2 fluxes ranged between 222 mgC m^{-2} d^{-1} and 1590 mgC m^{-2} d^{-1} (Table 2), with fluxes in each chamber varying by, on average, a factor of 2.5 ± 0.8.

The CO_2 fluxes of the chambers in the studied gully complex were broadly correlated with their elevation above the riverbed (Fig. 4). Chamber H2 recorded the highest fluxes, on average, while the chambers H4 and H7 had the lowest fluxes on average. Overall, the data reveal a positive relationship between CO_2 fluxes and the elevation of the chambers above the riverbed ($R^2 = 0.40$, $p = 0.005$, $n = 18$; Fig. 4). The correlation is weaker when the measurements made before the 03/05/2018 (first 3 days following the storm event) are excluded from this comparison ($R^2 = 0.25$, $p = 0.170$, $n = 9$).

The CO_2 fluxes were broadly linearly correlated with instantaneous air temperature at the start of each measurement ($R^2 = 0.17$, $p = 0.091$, $n = 18$; Fig. 5-A). This correlation is improved using the average temperature of the last 24 h before a measurement ($R^2 = 0.22$, $p = 0.049$, $n = 18$; Fig. 5B), and further improved when considering the measured ~2 h lag from the timing of the CO_2 flux measurement and the air temperature ($R^2 = 0.35$, $p = 0.010$, $n = 18$; Fig. 5C), based on the time lag observed between the air temperature record and the rock chambers (Fig. 3). The statistical outputs of the correlation between temperature and CO_2 flux do not vary notably when the lag time is between 1.5 h and 3 h. Furthermore, when the measurements made before the 03/05/2018 are excluded (first 3 days following the storm event) the correlation between CO_2 fluxes and air temperature is further improved ($R^2 = 0.67$, $p = 0.007$, $n = 9$; Fig. 5D).

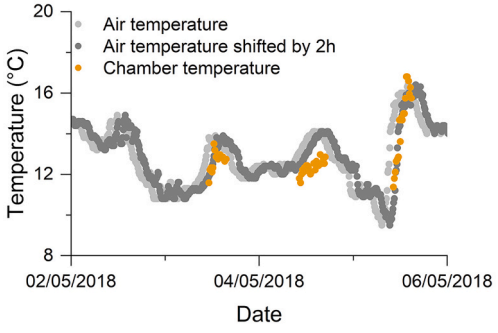

Fig. 3. Time series of air temperatures and chamber temperatures. Temperatures (°C) within the weathering chambers can be described by shifting the air temperature record from Poroporo Fire Station by 2 h.

Table 2
Summary table of CO_2 fluxes.

Chamber	Average flux (mgC m^{-2} d^{-1} ± σ)	Minimum flux (mgC m^{-2} d^{-1} ± σ)	Maximum flux (mgC m^{-2} d^{-1} ± σ)
H2	1125 ± 275 ($n = 5$)	758 ± 109	1590 ± 270
H3	662 ± 144 ($n = 4$)	544 ± 63	904 ± 97
H4	647 ± 219 ($n = 5$)	222 ± 2	834 ± 102
H5	731 ± 277 ($n = 3$)	441 ± 32	1105 ± 86
H7	611 ($n = 1$)	611 ± 60	611 ± 60

Standard deviations for the smallest and the largest flux measured at each chamber are reflecting the uncertainty of a single flux measurement, which consists of a series of repeated accumulations. The standard deviation for the average flux at each chamber is based on the average rate of accumulation for each flux measurement.

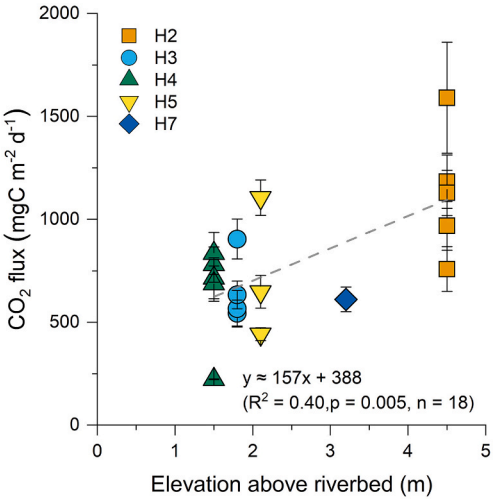

Fig. 4. Carbon dioxide flux from in situ weathering chambers versus their elevation above the riverbed. Fluxes [CO_2] (mgC m^{-2} d^{-1}) and their standard deviation are shown from five in situ weathering chambers as a linear function of the chamber elevation above the riverbed (m).

3.4. Rock chamber pCO_2

The measured rock pCO_2 varied between the gas accumulation chambers and over time (Fig. 2C). Overall, the pCO_2 values ranged between ~4700 ppmv and ~27,100 ppmv with an average temporal variability for a single chamber of a factor of 3.1 ± 1.6. Generally, the rock pCO_2 declined steadily following the storm event in all chambers although this trend is somewhat more evident for higher elevations above the riverbed (Fig. 2C). Furthermore, changes in rock pCO_2 correlate well with changes in CO_2 fluxes ($R^2 = 0.44$, $p = 0.004$, $n = 17$; Fig. 6).

3.5. Carbon isotope composition of CO_2

The stable carbon isotopic composition of the CO_2 sampled from the in situ weathering chambers revealed three samples with notably high $\delta^{13}C$ values, ranging from −5.5 ‰ to + 22.3 ‰. These samples were all collected 4 days after the chamber installation (02/03/2018 for H2 and H3, and 03/03/2018 for H5, respectively). The remaining samples had $\delta^{13}C$ values between −29.3 ‰ and −16.3 ‰.

Overall, these high $\delta^{13}C$ values correlate with a metric of excess carbon trapped on the molecular sieves. This is the ratio of the volume of CO_2 recovered from the zeolite molecular sieve cartridges (MSC), compared to that trapped based on the estimate of the volume of CO_2 loaded onto the sieves using the pCO_2 recorded with the infra-red gas analyzer ($IRGA_{CO2}$) (Fig. 7). This trend also reflects the time passed since the installation of each chamber. Together, this indicates the presence of

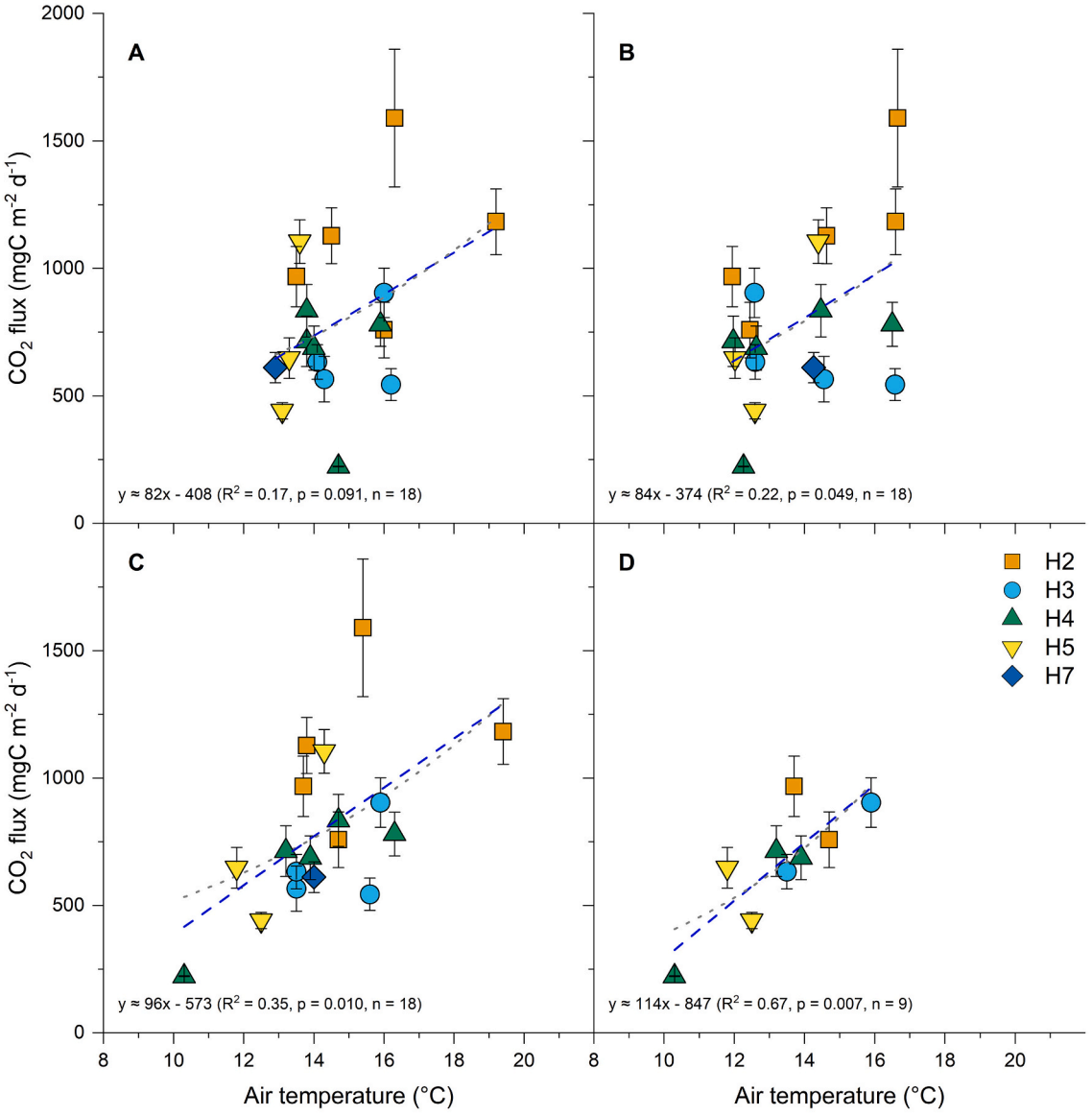

Fig. 5. Carbon dioxide flux versus temperature. Fluxes [CO_2] (mgC m^{-2} d^{-1}) and their standard deviation are shown from five in situ weathering chambers as a function of the air temperature record from Poroporo Fire Station treated in different ways: A) All CO_2 flux measurements versus the air temperature at the start of each measurement. B) All CO_2 flux measurements versus the average air temperature over the last 24 h of a measurement. C) All CO_2 flux measurements versus the air temperature delayed by 2 h from the timing of each measurement. D) CO_2 flux measurements without measurements made before the 03/05/2018 (excluding the first 3 days following the storm event) versus the air temperature delayed by 2 h from the timing of each measurement. Details of linear functions (dashed blue lines) are given in each panel. As an alternative (Section 4.2.2), exponential functions (dotted gray lines) are delineated in the background.

a contaminant in the trapped gases of the initial samples that was not detected by the IRGA as CO_2 but that behaves in a similar way to CO_2 during the CO_2 recovery and purification in the laboratory. Laboratory experiments following the field trip identified that the silicone sealant used was the source of some contamination, releasing an unidentified gas during the curing process that interferes heavily on the IRMS (at *m/z* value 45). However, it was found that curing finishes mostly within 3 days and that no contamination of the stable carbon isotope measurement occurs when the sealant has dried for 1 week under outside conditions similar to the field setup.

Therefore, only CO_2 sampled from the end of the fieldtrip is used for further interpretations in this study. In contrast, the CO_2 volumes and $\delta^{13}C$ values of samples collected before the sealant dried are tainted and likely to be only an apparent signal consisting of naturally emitted CO_2 and the contaminant (Fig. 7). It is important to note that the CO_2 flux measurements are not affected by the contaminant.

Stable carbon isotope analyses revealed a $\delta^{13}C$ of −29.3 ‰ for CO_2 collected from chamber H3 on the 04/05/2018 (6 days after the installation) and a $\delta^{13}C$ of −28.3 ‰ for the following day. The radiocarbon activities for this CO_2 from chamber H3 were $F^{14}C = 0.0122 \pm 0.0049$ and $F^{14}C = 0.0547 \pm 0.0047$, respectively (Table 3). The radiocarbon content is used to assess the contributions from the atmosphere (mass fraction; f_{Atm}) and from petrogenic carbon (that is the combined pool of inorganic and organic carbon; $f_{Petrogenic\ C}$) to the sampled gases by solving the following isotope mass balance system:

$$f_{Atm} + f_{Petrogenic\ C} = 1$$

$$f_{Atm} \times F^{14}C_{Atm} + f_{Petrogenic\ C} \times F^{14}C_{Petrogenic\ C} = F^{14}C_{Chamber}. \quad (5)$$

Based on the assumption that the declining trend of the atmospheric radiocarbon content over the last few decades can be described by a linear regression (Cerling et al., 2016; Hua et al., 2013), we estimate the

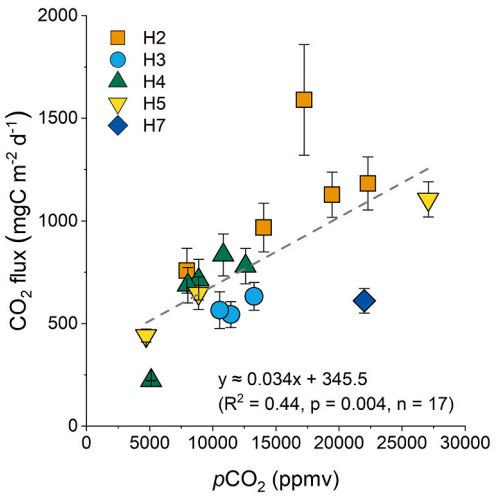

Fig. 6. Carbon dioxide flux versus partial pressure of carbon dioxide in the weathering zone. Partial pressures [pCO_2] (ppmv), representative for the storage of CO_2 in a gas accumulation chamber and surrounding rock pores prior to a flux measurement, are correlated with CO_2 fluxes from five in situ weathering chambers. Standard deviations are given for CO_2 flux measurements while the standard deviation of a single pCO_2 measurement cannot be determined with the applied method.

radiocarbon content of the local atmospheric CO_2 to be $F^{14}C_{Atm} = 1.0216$ during the sampling period, by extrapolating an atmospheric record of radiocarbon dioxide measurements from Wellington, New Zealand, for the years 2013–2017 (Turnbull et al., 2017). This estimated value is close to the latest report of $F^{14}C = 1.0226$ for 20/09/2017 (Turnbull et al., 2017). Correcting for the atmospheric contributions ($f_{Atm} \approx 1.2\%$ and 5.4%, respectively) by taking its $\delta^{13}C_{Atm}$ value of −8.6 ‰ into account indicates that the petrogenic carbon pools in the two CO_2 samples have very similar $\delta^{13}C$ signatures ($\delta^{13}C_{Petrogenic\ C}$) of −29.5 ± 0.1 ‰ within the measurement uncertainties (Table 3), following the equation

$$f_{Atm} \times \delta^{13}C_{Atm} + f_{Petrogenic\ C} \times \delta^{13}C_{Petrogenic\ C} = \delta^{13}C_{Chamber}. \quad (6)$$

Since the radiocarbon activities of the sampled CO_2 are very low, we estimate any uncertainty of the atmospheric correction that is associated with extrapolating the atmospheric radiocarbon content to be negligible.

4. Discussion

4.1. Source of rock-derived CO_2

To quantify the CO_2 emissions from weathering of mudstones exposed in the Waiapu catchment (Fig. 1), it is crucial to first constrain the source of carbon. To do this, we rely on the stable and radioactive

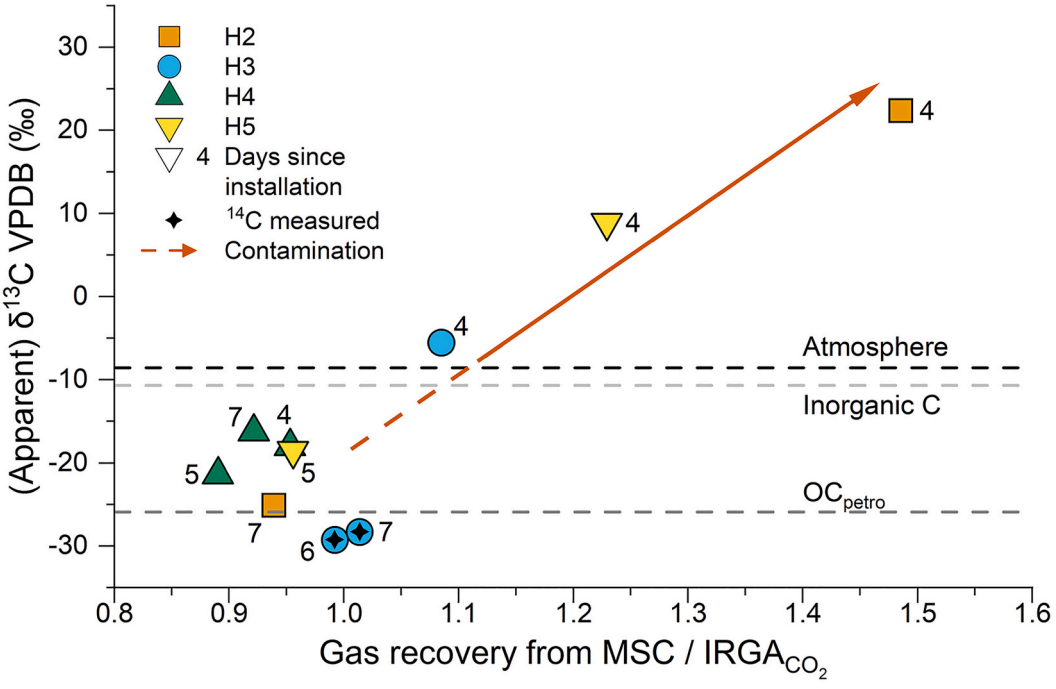

Fig. 7. Stable carbon isotope measurement of CO_2 from in situ weathering chambers versus sampling efficiency. Excess of gas recovered from the molecular sieve cartridges (MSC) compared to the amount of CO_2, which theoretically should have been trapped in the field according to the infra-red gas analyzer (IRGA), correlates with the $\delta^{13}C$ (‰ VPDB) of the sample. This trend coincides with the time passed since the installation of the particular chamber, which is denoted next to each data point (days), indicating a contamination of the trapped CO_2 associated with the chamber set-up. This contaminant is not detected by the IRGA (i.e., does not impact CO_2 flux measurements) but behaved similar to CO_2 during the CO_2 recovery and purification in the laboratory, and interferes heavily on isotopic measurements. An uncontaminated sample has typically a sampling efficiency of ~95% with the applied methods.

Table 3
Carbon isotope composition of sampled CO_2.

Sample	Date	Publication code	$\delta^{13}C$ (‰ VPDB ±0.1)	Fraction modern (± 1σ)	$\delta^{13}C$ (‰ VPDB ±0.1) corrected for atm. contribution
Atmosphere	03/05/2018	–	−8.6	1.0216*	–
H3	04/05/2018	SUERC-84238	−29.3	0.0122 ± 0.0049	−29.6
H3	05/05/2018	SUERC-84239	−28.3	0.0547 ± 0.0047	−29.4

The atmospheric contributions to chamber H3 are corrected using an extrapolated fraction modern based on a published record for the years 2013–2017 (Turnbull et al., 2017) (*).

carbon isotopic composition of the emitted CO_2, which is used alongside measurements of the rocks undergoing weathering. This allows us to track the contributions from OC_{petro}, carbonates and the atmosphere. The very low radiocarbon content of the sampled CO_2 ($F^{14}C$ = 0.0122–0.0547) indicates only minor contributions from modern atmospheric CO_2 (f_{Atm} <6%), and also confirms the underlying assumption that neither soil organic matter nor plants incorporating modern carbon contribute any CO_2 in the rock outcrops we studied (Fig. 1).

The mudstones that make up the study site contain very little inorganic carbon (IC) as disseminated carbonate (<0.2 wt%). The OC_{petro}/IC ratio is ≥4.5. This could suggest that the contribution of IC to the CO_2 emissions via reaction 2 is negligible in this setting. Indeed, the $\delta^{13}C$ values of trapped CO_2 (~−29.5 ‰, corrected for atmospheric contribution; Table 3) confirm this hypothesis because they are significantly more negative than that of typical Cretaceous marine carbonates (~0 ‰ to + 5 ‰) (Erba, 2004; Gröcke et al., 2003; Weissert et al., 1998) or that of IC from the study site (−10.7 ‰). This contrasts notably with the carbonate-rich marly rocks of the Laval catchment in the Draix-Bléone Critical Zone Observatory (CZO; France) where carbonate dissolution by sulfuric acid derived from the oxidation of sulfide minerals (Reaction 2) contributes >70% of the emitted CO_2 (Soulet et al., 2021, 2018). However, we do not exclude that carbonate dissolution could contribute to the carbon fluxes from weathering in the Waiapu catchment because carbonate concretions are a common feature in several outcropping lithologies (Mazengarb and Speden, 2000; Speden, 1976) and dissolved ion fluxes suggest high carbonate weathering rates (Lyons et al., 2005).

The $\delta^{13}C$ values of CO_2 from our accumulation chambers are more negative than the $\delta^{13}C$ values of OC_{petro} (−25.9 ‰) in rock samples. Having corrected for carbon input from atmospheric CO_2, the offset is ~3.6 ‰ (Table 3). It is important to note that previous work did not find any carbon isotope fractionation associated with the methods used for gas sampling and processing while testing CO_2 standards with volumes similar to our samples (Garnett et al., 2019; Hardie et al., 2005). In addition, any contamination of the trapped gases associated with the setup of the accumulation chambers (silicone sealant) is avoided by considering samples collected approximately 1 week after installation (Fig. 7). Indeed, if present, such a contamination would lead to an apparently heavier stable carbon isotope composition and thus could not explain the lower $\delta^{13}C$ values of emitted CO_2 compared to OC_{petro}. In addition, the $\delta^{13}C$ values of OC_{petro} reported here are verified by comparison with previous work in the Waiapu catchment (Thompson, 2009). Therefore, we explore two remaining scenarios for why the $\delta^{13}C$ signatures of CO_2 from mudstone weathering are offset from OC_{petro}: i) an additional fossil carbon source with a more negative $\delta^{13}C$ value; and/or ii) carbon isotope fractionation associated with the weathering processes.

4.1.1. Metamorphic contributions of CO_2 and CH_4 oxidation

One explanation for the ^{13}C-depleted nature of the sampled CO_2 compared to the $\delta^{13}C$ values of the OC_{petro} in the mudstones could be contributions of CO_2 or methane (CH_4) that is oxidized to CO_2 below (or around) the accumulation chambers from deeper belowground sources. In general, during metamorphism of sedimentary rocks, the thermal decomposition of OC_{petro} and/or decarbonation of carbonate minerals can release CO_2 and CH_4 (Evans et al., 2008; Hoefs and Frey, 1976), both to variable extents, with their abundances controlling their carbon isotope compositions (Evans et al., 2008; Giggenbach, 1997; Menzies et al., 2018). In the northeast of New Zealand, gas seeps occasionally occur but none are reported in close proximity to our study site (Francis et al., 1991; Reyes et al., 2010; Scadden et al., 2016). In the wider area, the composition of gas discharged from springs indicates that CO_2 and CH_4 are close to or in a thermally controlled isotopic equilibrium (Giggenbach et al., 1995). While a metamorphic carbon source would most likely be ^{14}C-free, CO_2 from spring water in the region has high $\delta^{13}C$ values of ~−12.0 ‰ (ranging from −6.7 ‰ to −17.3 ‰) which is ~17.5 ‰ more positive than the $\delta^{13}C$ values of CO_2 that we sampled (Giggenbach et al., 1995; Lyon and Giggenbach, 1992). Thus, even if missed, a metamorphic CO_2 source could not explain our observations.

Gas in waters from cold and hot springs in the northeast of New Zealand can be dominated by thermogenic CH_4 and only contain trace amounts of CO_2 (Giggenbach et al., 1993; Lowry et al., 1998). Taking into account the reported $\delta^{13}C$ values of CH_4 of −34 ‰ to −42 ‰ for this area (Giggenbach et al., 1995; Lyon and Giggenbach, 1992) and a carbon isotope fractionation during aerobic or anaerobic methane oxidation of 5–30 ‰ (Whiticar, 1999), a CH_4 source that is oxidized and degassing into our chambers would have a $\delta^{13}C$ value of CO_2 between −39 ‰ and −72 ‰. If oxidation of thermogenic CH_4 was occurring, this process alone cannot explain the measured $\delta^{13}C$ values of chamber CO_2. Instead, we would have to invoke a mixture with contributions from an isotopically heavier source (e.g., OC_{petro}). However, to shift the CO_2 stable isotopic composition by 3.6 ‰, we calculate that the mass of thermogenic CH_4 flux would have to be very large, ranging from ~62 mgC m^{-2} d^{-1} to ~218 mgC m^{-2} d^{-1}, and represent 7.8–27.4% of the average CO_2 release from the chambers (795 mgC m^{-2} d^{-1}). This would be similar in size to the globally highest CH_4 fluxes from sub-tropical wetland soils (Oertel et al., 2016). Furthermore, it would greatly exceed the mean CH_4 flux of ~6 mgC m^{-2} d^{-1} from microseepage in soils over near-surface oil-gas reservoirs or active geothermal areas (Etiope and Klusman, 2010). Indeed, it would be comparable only to the highest fluxes associated with macro-seeps in such settings (Etiope and Klusman, 2010, 2002). Thus, a significant metamorphic carbon contribution to the CO_2 emissions measured in our accumulation chambers appears to be unlikely.

4.1.2. Microbial impact on OC_{petro} oxidation and carbon isotope fractionation

An alternative explanation for the $\delta^{13}C$ values of the CO_2 would be via carbon isotope fractionation associated with microbial heterotrophic respiration (Petsch et al., 2001), which can produce CO_2 that is ^{13}C-depleted compared to the substrate (Blair et al., 1985; Werth and Kuzyakov, 2010). However, although previous studies have shown that microorganisms can thrive aerobically on OC_{petro} as a sole carbon source (Matlakowska and Sklodowska, 2011; Petsch et al., 2001; Stasiuk et al., 2017), to our knowledge, no report exists yet on carbon isotope fractionation during the CO_2 release from microbial degradation of OC_{petro}. In contrast, this process is well described for soil organic matter. As reviewed by Werth and Kuzyakov (2010), the ^{13}C-depletion in soil microbial respiration is an apparent isotope fractionation as the combined result of three effects: i) kinetic ^{13}C-fractionation; ii) preferential substrate utilization; and iii) heterogeneity and activity of microorganisms. The ~3.6 ‰ ^{13}C-depletion of CO_2 emissions compared to OC_{petro} reported here is well within range of the kinetic carbon isotope fractionation during microbial catabolism, leading to a ^{13}C-depletion in respired CO_2 that is balanced typically by a 0.1–5.7 ‰ ^{13}C-enrichment of the microbial biomass in soils (Blair et al., 1985; Šantrůčková et al., 2000).

Thus, our measurements would be consistent with a microbial process that leads to a ^{13}C-depletion in CO_2 produced during oxidative weathering. However, further research is needed to constrain the detail and magnitude of the offsets. Ramped temperature pyrolysis or oxidation, coupled with stable carbon analysis, could be used to determine whether ^{13}C-depleted fractions of OC_{petro} are oxidized preferentially (Hemingway et al., 2018, 2017). This signature may be present in organic biomarkers associated with microbial activity (e.g., phospholipid fatty acids) (Petsch et al., 2001; Schwab et al., 2019; Seifert et al., 2013, 2011). Modification of OC_{petro} oxidation experiments (Chang and Berner, 1999) could also be informative, when coupled to an apparatus to measure the isotopic composition of evolved gases (Beaupré et al., 2016). In summary, we conclude that the oxidation of OC_{petro} is the sole contributor of CO_2 in this case, with lower $\delta^{13}C$ values of the CO_2 possibly relating to isotopic fractionation associated with microbial respiration of OC_{petro} during weathering.

4.2. Rock-derived CO_2 fluxes and their environmental controls

In general, the large CO_2 emissions from oxidative weathering of OC_{petro} in mudstones of northern New Zealand have a similar magnitude as fluxes from soil respiration reported for various soil types and climates (Oertel et al., 2016; Raich and Schlesinger, 1992). Furthermore, they are comparable in size to OC_{petro}-derived CO_2 fluxes measured in marly rocks exposed in the French Alps ranging from ~1 mgC m^{-2} d^{-1} to ~790 mgC m^{-2} d^{-1}, although at the French site the OC_{petro}-derived CO_2 fluxes are ~5.5 times lower than CO_2 fluxes from carbonate dissolution (Soulet et al., 2021). Both locations experience very high erosion rates. In the Waiapu catchment, the sediment export rates are ~17,800 t km^{-2} yr^{-1} (Betts et al., 2003; Hicks et al., 2004), whereas in the Laval catchment in the Draix-Bléone CZO they are ~11,200 t km^{-2} yr^{-1} (Mathys et al., 2003). Estimates of OC_{petro} oxidation using the rhenium-proxy suggest that high erosion rates could sustain rapid rates of oxidation (Hilton et al., 2014), and this could explain the apparent, broad similarity between the sites. We also note that the rocks in the Waiapu River basin contain slightly more OC_{petro} (0.76 wt%) than the rocks in the Laval catchment (~0.54 wt%) (Soulet et al., 2021), but again they are broadly similar. These features are interesting and call on more studies that quantify OC_{petro} oxidation and their CO_2 emissions in this way. However, to make more detailed comparisons requires a larger dataset than is presently available. Here, instead, we focus on the observation that OC_{petro} fluxes appear to respond quickly to environmental changes.

4.2.1. Local topographic position and moisture

The relationship between CO_2 fluxes and the elevation of the chambers above the riverbed (Fig. 4) can be explained in terms of diffusive processes operating in a hydrological framework. The degree of water-saturation generally decreases with increasing elevation above the riverbed (Lu and Godt, 2013; Mason et al., 2016), which allows for more diffusive exchange of any connected pore space around the chamber (Bao et al., 2017; Bolton et al., 2006; Feng et al., 2002; Tremosa et al., 2020; Voroney and Heck, 2015). This provides greater amounts of oxygen for the oxidation of OC_{petro} (Reaction 1), and, if present, the oxidation of pyrite that can lead to dissolution of carbonate minerals (Reactions 2 and 3). Furthermore, lower degrees of water-saturation in the weathering zone increase the amount of CO_2 that escapes in gaseous form while the export of dissolved inorganic carbon to the river decreases (Hasenmueller et al., 2015; Neu et al., 2016; Tune et al., 2020). These inferences offer an explanation for the relationship between chamber elevation and CO_2 flux (Fig. 4), and confirm findings from the French Alps where five gas accumulation chambers were installed within 2.5 m elevation above a riverbed (Soulet et al., 2021).

Another way to examine these controls is to categorize our data set into "wet" and "dry" measurement periods. We do this based on a threshold of 3 days after the rain event (Fig. 2A). This categorization indicates the hydrological control on CO_2 fluxes since their correlation with the chamber elevation is lower when "wet" samples are excluded ($R^2 = 0.40$ and $R^2 = 0.25$, respectively). This also affects the pCO_2 within the weathering zone (Fig. 2C) similar to findings in soils where high levels of moisture act as a diffusion barrier that leads to greater accumulations of CO_2 (Hasenmueller et al., 2015). However, future research is needed to specify the impact of the hydrology in the shallow weathering zone on the production and accumulation of CO_2.

Previous studies have indicated that the presence of water is crucial for microbial life in the weathering zone. In the laboratory, dissolved OC_{petro} derived from an aqueous kerogen dissolution can be rapidly assimilated and biodegraded by aerobic heterotrophic bacteria (Schillawski and Petsch, 2008). The authors suggested that the dissolution could be the rate limiting step of respiration of OC_{petro}. Furthermore, recent research highlighted the importance of aqueous subaerial biofilms for the degradation of OC_{petro}, which act to incorporate enzymes crucial for aerobic heterotrophic metabolism (Stasiuk et al., 2017). Taken together, this could mean that the CO_2 fluxes from OC_{petro} oxidation relate to moisture in a bell-shaped curve. At low levels of moisture, CO_2 production is inhibited due to a lack of an aqueous transport and reactant medium that is also needed to create epilithic biofilms. At high levels of moisture, the CO_2 production is hampered due to a limited oxygen supply.

4.2.2. Temperature

Our 6 day measurement period revealed a positive relationship between CO_2 flux from OC_{petro} and regional air temperatures (Fig. 5). Daily-averaged air temperatures indicate a broadly positive relationship. However, the correlation is stronger when considering a 2 h lag between the measurements and air temperature record (Fig. 5C). This time lag was observed between the local climate station and the rock chambers (Fig. 3) and is likely associated with thermal diffusion in the probed weathering zone. Minor variability in the time lag over the study period can be expected based on the control of the water content in the pore space on the overall thermal conductivity (Hopmans et al., 2002; Romio et al., 2019), which may result in an uncertainty of up to 50% on the time lag. However, this uncertainty does not significantly impact the quality of the relationship between CO_2 flux and temperature. This is also true for the improvement of the correlation when "wet" measurements are excluded (Fig. 5D). Despite the influence of precipitation and of the topographic position of the chambers on the CO_2 fluxes, the evidence for an important temperature control on the oxidative weathering of OC_{petro} is unambiguous. It should be noted that single chambers respond comparably to temperature, such as H3 and H4 located at similar elevation above the riverbed, and the trend of this relationship is confirmed by comparing the combined CO_2 fluxes of all chambers with the temperature record (Fig. 5).

Previous research has indicated the presence of such an environmental control by investigating the oxidation of coal in laboratory experiments but this was restricted to two temperatures at 24 °C and 50 °C (Chang and Berner, 1999). Only recently, seasonal investigations of in situ oxidative weathering of OC_{petro} contained in marly rocks have specified this relationship as highly sensitive and exponential (Soulet et al., 2021). To provide an exponential measure of the change in flux as the consequence of increasing the reaction temperature by 10 °C, a dimensionless Q_{10} value can be calculated:

$$Q_{10} = exp(10\ ^{\circ}C \times \alpha), \tag{7}$$

where α is the growth rate parameter ($^{\circ}C^{-1}$) that can be derived from a growth exponential model:

$$F = F_0 \times exp(\alpha \times T), \tag{8}$$

where F is the CO_2 flux (mgC m^{-2} d^{-1}), T is the temperature (°C) and F_0 is the CO_2 flux at 0 °C. The Q_{10} coefficient of Soulet et al. (2021) can be compared with our dataset, although we note that the data from the Waiapu basin can be described sufficiently by a linear relation (Fig. 5). By using an exponential model, we find a Q_{10} value of 2.7 ± 1.0 (F_0 = 195 ± 108 mgC m^{-2} d^{-1}; ± standard error; $R^2 = 0.30$, $p < 0.001$, n = 18), based on the air temperatures delayed by 2 h (Fig. 5C). Interestingly, this is similar, albeit slightly higher, to the OC_{petro} oxidation Q_{10} value of 2.2 ± 0.5 reported for the Laval catchment, based on daily-averaged chamber temperatures (Soulet et al., 2021). It is well within the global range of CO_2 fluxes from soil respiration with a mean Q_{10} value of 3.0 ± 1.1 for the 0–20 °C temperature range (Bond-Lamberty and Thomson, 2010). However, when considering only the "dry" fluxes (Fig. 5D), which were measured in the range of around 10–16 °C, the Q_{10} temperature coefficient is higher, at 4.8 ± 2.5 ($R^2 = 0.61$, $p < 0.001$, n = 9).

The similarity of Q_{10} values of petrogenic CO_2 fluxes and of soil respiration suggests a microbial control on the kinetics of the oxidation of OC_{petro}, analogous to soils (Bond-Lamberty and Thomson, 2010; Oertel et al., 2016). Since microbial enzymes have the potential to

increase the rate of breakdown of organic matter by several orders of magnitude, small changes in microbial activity (e.g., by changes in humidity) have the potential to induce large changes in the associated CO_2 production (Leifeld and von Lützow, 2014). The number of enzymatic steps that are required to release a carbon atom from organic matter as CO_2 is assumed to depend on its reactivity, which in turn is controlled by various factors such as solubility, molecular size and functionalization, and association with fine-grained minerals (Bosatta and Ågren, 1999; Schmidt et al., 2011). Accordingly, it can be expected that oxidative weathering of OC_{petro} depends not only on environmental and microbial variables but also on the characteristics of the organic matter and its surrounding rock matrix (i.e., its mineral association) (Hemingway et al., 2019). This could explain differences in CO_2 emissions in contrasting lithologies. Overall, as highlighted by Soulet et al. (2021), our Q_{10} value identifies oxidative weathering of OC_{petro} as a positive feedback to warming, most relevant to the geological carbon cycle. At present, models of chemical weathering fluxes in the geological carbon cycle do not attempt to parametrize OC_{petro} oxidation with a temperature control (Caves Rugenstein et al., 2019; Isson et al., 2020) and the measurements here support the finding of Soulet et al. (2021) that this modification is necessary.

4.3. Wider implications for understanding Earth's carbon cycle

We have identified the oxidation of OC_{petro} as the source of rapid rates of CO_2 release measured in rock outcrops of the Waiapu catchment. We find environmental controls on these fluxes that are analogous to those reported in a setting with contrasting bedrock (Soulet et al., 2021, 2018). Thus, we propose that the studied gully complex should not only be representative of a large portion of the Waiapu catchment and neighboring watersheds in New Zealand (Gomez et al., 2004; Hicks et al., 2000; Leithold et al., 2006; Mazengarb and Speden, 2000; Thompson, 2009), but also for similar lithologies in rapidly eroding settings elsewhere. However, future research is needed to investigate contrasting lithologies, for example, in respect to differences in the mechanical state of the bedrock that may impact the reacting surface areas and the diffusive movement of CO_2 and O_2 in the weathering zone (Gu et al., 2020).

4.3.1. Feasibility of short-term investigations to reveal environmental controls on rock-derived CO_2 fluxes

There have been only two studies that attempt to establish long-term records (months to years) of directly measured rock-derived CO_2 fluxes to help constrain their environmental controls (Keller and Bacon, 1998; Soulet et al., 2021, 2018). Using gas sampling wells over ~7 m depth in shallow soil underlain by glacial till dominated by shales, Keller and Bacon (1998) provided the first in situ evidence for petrogenic CO_2, differentiating it from soil respiration over a 1-year period at monthly intervals. More recently, at the Draix-Bléone CZO, CO_2 flux measurements were made on seasonal visits over 2.5 years (Soulet et al., 2021) from rock chambers drilled into rock outcrops undergoing weathering (the design used in this study).

Here, we show that the design for in situ CO_2 measurements of Soulet et al. (2018) can be applied in stand-alone investigations without a conceptual framework of repeated visits. The potential to capture significant short-term changes in temperature and hydrology, which can be linked to changes in CO_2 fluxes (Figs. 2B and 5), was previously indicated by findings in the Draix-Bléone CZO (Soulet et al., 2021). The approach used in this study is feasible even in remote locations. The general location of the field site was explored from remote sensing imagery prior to fieldwork. The first 2 days of the trip were used to search for a suitable location within the study area and install the chambers (using only portable drilling equipment). At the end of the measurement period, the setup can be easily dismantled within a few minutes and all material removed from the environment. To exclude the possibility of contamination of the molecular sieves used for trapping the CO_2, we recommend starting CO_2 collection approximately 1 week after the chamber setup when using a sealant containing drying agents (Fig. 7). In the future, automation of the flux measurements, for instance using electrically-actuated valves, could allow several recordings in parallel and provide further detail in the dataset.

One drawdown of a stand-alone trip is the limited range in environmental variables that can be observed, which could potentially be extended significantly by repeated visits over various seasons (depending on the seasonality in the study area), as performed in the Draix-Bléone CZO (Soulet et al., 2021). Nevertheless, our work shows that short field campaigns are viable and provide new insight on the environmental controls on OC_{petro} oxidation for a given substrate. This approach can now be used to study in situ CO_2 emissions and their controls across climatic, lithological and biological variables.

4.3.2. Rock pCO_2 and silicate weathering

The oxidation of OC_{petro} in the critical zone also bears relevance to other chemical weathering processes because it can influence the partial pressure of CO_2 within the weathering zone. At our study site in the Waiapu catchment, the temperature and humidity combine to control the accumulation of CO_2 within the chambers (Figs. 4 and 5), and thus the pCO_2 in the surrounding rock pores (Fig. 6). Since the sampled mudstones have low inorganic carbon contents (<0.2 wt%), the consumption of CO_2 produced by OC_{petro} oxidation cannot be negated by the dissolution of carbonate minerals as it would in carbonate-rich lithologies (Calmels et al., 2014). In contrast, the high pCO_2 values that we measured could have the strong potential to drive the weathering of co-occurring silicate minerals, which can contain >25 wt% feldspar (mostly plagioclase) and 15 wt% chlorite (Kenny, 1984), by acid-hydrolysis reactions. In this process, a high pCO_2 is expected to be associated with a low pH, which facilitates the dissolution of silicate minerals by carbonic acid, which itself is transformed into bicarbonate (Drever, 1994; Ebelmen, 1845). The dissolution should be further amplified by organic acids formed by microorganisms during the breakdown of OC_{petro} as it is within soils (Stasiuk et al., 2017; Waksman and Starkey, 1931).

We found that almost all the CO_2 within the pore space of the studied mudstones in the Waiapu River gully complex is rock-derived. Thus, atmospheric CO_2 is not likely to have been involved in any silicate weathering reactions in the shallow subsurface of these bare rock outcrops. There, chemical weathering of silicate minerals cannot act as an atmospheric CO_2 sink mechanism (Berner, 1999; Gaillardet et al., 1999; Moon et al., 2014). Instead, rock-derived carbon that is transformed during silicate weathering is likely to be exported by the Waiapu River as bicarbonate. This may be released as CO_2 during river transport (Raymond et al., 2013), and/or eventually precipitate as $CaCO_3$ in the oceans (Berner, 1999; Walker et al., 1981). If the newly precipitated carbonates form from carbon originally derived from OC_{petro}, their formation would represent no modern-day carbon transfer to the carbonate mineral. In fact, half of the exported bicarbonates would return to the atmosphere as CO_2 based on the stoichiometry of this process (Berner, 1999). This would minimize the overall carbon sink linked to silicate weathering in locations that share similarities with our studied setting, with high erosion rates, sedimentary rocks and oxidative weathering (Bufe et al., 2021). Furthermore, this would also mean that the dissolved cations derived from silicate weathering, which are transferred from similar weathering zones into the Waiapu River, could in fact be linked back to oxidative weathering of OC_{petro}.

For the study area, we can explore this further using our one-time estimates of OC_{petro} oxidation to compare with those of silicate weathering and carbonate weathering. There are several caveats to be noted here. First, our chamber-based measurements show systematic variation between chambers (linked to their topographic position; Fig. 4) and within a chamber over 6 days due to ambient temperature and precipitation conditions (Fig. 2). Therefore, it is difficult to provide an estimate of flux that would be representative of a longer-term flux. Second, it is

unclear in how far weathering fluxes in less erosive settings (e.g., with pronounced soil and vegetation cover), which are present in the wider area (Fig. 1), differ from those in highly erosive settings similar to the study site. Furthermore, we normalize the measured fluxes to the chambers internal area, which allows chambers to be compared meaningfully. However, this is not the same as normalizing fluxes to the surface area exposed in a catchment (Soulet et al., 2021). Finally, the published silicate and carbonate weathering fluxes for the Waiapu catchment are based on only a single assessment (Lyons et al., 2005). Nevertheless, the comparison is informative. The published CO_2 drawdown associated with silicate weathering is 5.7×10^5 mol CO_2 km^{-2} yr^{-1}, which translates to an average of ~18.8 mgC m^{-2} d^{-1} over the catchment area. Similarly, the carbonate weathering flux is 1.2×10^5 mol CO_2 km^{-2} yr^{-1}, which translates to an average of ~4 mgC m^{-2} d^{-1}. These catchment-wide estimates are much lower than the OC_{petro} oxidation fluxes we measured in chambers of the gully complex, which ranged from 222 mgC m^{-2} d^{-1} to 1590 mgC m^{-2} d^{-1} (Table 2). Depending on the wider rates of OC_{petro} oxidation that occur throughout the catchment, for which trace metal proxies such as rhenium in river water could shed light (Hilton et al., 2014), it appears that the CO_2 supply from OC_{petro} oxidation could play a major role in silicate and carbonate weathering fluxes by carbonic acid in this type of setting.

Overall, a direct impact of the oxidation of OC_{petro} on silicate and/or carbonate dissolution suggests that differentiating the carbon cycle into a silicate-carbonate subcycle and an organic matter subcycle as it has been suggested by Berner (1999) oversimplifies the complexity of chemical weathering and calls for a more holistic view. Together with identifying the carbon sources associated with oxidative weathering, the parallel dissolution of silicate minerals needs to be considered in any overall assessment of chemical weathering of sedimentary rocks (Blattmann et al., 2019; Bufe et al., 2021; Hilton and West, 2020; Jin et al., 2014). However, while the high rock-derived CO_2 fluxes and pCO_2 values identify the mudstones studied here as a clear carbon source, future research is needed to constrain weathering pathways at larger scales, and through the inorganic carbon pool of river catchments.

5. Conclusions

We have measured CO_2 release during weathering of mudstones in the Waiapu catchment, New Zealand, using a short-term installation of accumulation chambers installed directly into exposed rock outcrops. They reveal rapid instantaneous fluxes that range from 222 mgC m^{-2} d^{-1} to 1590 mgC m^{-2} d^{-1} over the study period of 6 days. The setting experiences rapid erosion rates, and these measurements confirm that steep mountain catchments comprised of sedimentary rocks can act as hotspots of carbon cycling between the lithosphere and the atmosphere.

Based on the magnitude of the CO_2 fluxes and the stable and radioactive carbon isotopic composition of CO_2 sampled from the chambers, OC_{petro} is the sole contributor of carbon in this setting. There is a depletion of ~3.6 ‰ in the $\delta^{13}C$ values of CO_2 when compared to OC_{petro} in rocks. We suggest this may reflect carbon isotope fractionation associated with microbial respiration of OC_{petro}. In addition, CO_2 fluxes responded quickly to changes in temperature and humidity. Together, this supports the importance of environmental controls on chemical weathering and climate change feedbacks.

We measured very high pCO_2 in the shallow weathering zone of these rock outcrops, with negligible input from atmospheric CO_2. This high pCO_2 could induce the weathering of silicate minerals using the rock-derived CO_2. Any subsequent transfer of carbon in the bicarbonate pool of rivers would represent a leak of carbon derived from OC_{petro} oxidation to the atmosphere elsewhere, and the local silicate weathering would not act as an atmospheric CO_2 sink. This suggests the need to consider a direct connection of OC_{petro} oxidation and silicate weathering in rapidly eroding mudstones, and for how these play out in the wider carbon cycle. Overall, this study provides a framework for future work regarding a better understanding of the chemical weathering of sedimentary rocks and their climatic, lithological and biological interrelations which can now be addressed with short field campaigns even in remote areas following the presented methodology.

Data availability

All data that support the findings of this study are available from the Natural Environment Research Council (NERC, UK) – Environmental Data Service (EDS) National Geoscience Data Centre with the identifier DOI: https://doi.org/10.5285/467fcf54-eb20-4a19-a62d-8867516de87c.

Declaration of Competing Interest

The authors declare that they have no known competing financial interests or personal relationships that could have appeared to influence the work reported in this paper.

Acknowledgements

This work was supported by the European Research Council (Starting Grant to RGH, ROC-CO2 project, grant 678779). We thank M. A. Barton and H. Roil for permission to access the field site, M. Dellinger and M. Ogrič for field assistance, C. Delport and D. R. Gröcke for assistance with data acquisition, and T. Blattmann and one anonymous referee for comments which improved the manuscript.

References

Bao, Z., Haberer, C.M., Maier, U., Amos, R.T., Blowes, D.W., Grathwohl, P., 2017. Modeling controls on the chemical weathering of marine mudrocks from the Middle Jurassic in Southern Germany. Chem. Geol. 459, 1–12. https://doi.org/10.1016/j.chemgeo.2017.03.021.

Bardgett, R.D., Richter, A., Bol, R., Garnett, M.H., Bäumler, R., Xu, X., Lopez-Capel, E., Manning, D.A.C., Hobbs, P.J., Hartley, I.R., Wanek, W., 2007. Heterotrophic microbial communities use ancient carbon following glacial retreat. Biol. Lett. 3, 487–490. https://doi.org/10.1098/rsbl.2007.0242.

Beaupré, S.R., Mahmoudi, N., Pearson, A., 2016. IsoCaRB: a novel bioreactor system to characterize the lability and natural carbon isotopic (14C, 13C) signatures of microbially respired organic matter. Limnol. Oceanogr. Methods 14, 668–681. https://doi.org/10.1002/lom3.10121.

Bergman, N.M., Lenton, T.M., Watson, A.J., 2004. COPSE: a new model of biogeochemical cycling over Phanerozoic time. Am. J. Sci. 304, 397–437. https://doi.org/10.2475/ajs.304.5.397.

Berlendis, S., Beyssac, O., Derenne, S., Benzerara, K., Anquetil, C., Guillaumet, M., Estève, I., Capelle, B., 2014. Comparative mineralogy, organic geochemistry and microbial diversity of the Autun black shale and Graissessac coal (France). Int. J. Coal Geol. 132, 147–157. https://doi.org/10.1016/j.coal.2014.07.005.

Berner, R.A., 1999. A New look at the long-term Carbon Cycle. GSA Today 9, 1–6.

Berner, R.A., 2004. The Phanerozoic Carbon Cycle. Oxford University Press, New York, USA.

Berner, E.K., Berner, R.A., 2012. Global Environment: Water, Air, and Geochemical Cycles, 2nd ed. Princeton University Press, New Jersey, USA.

Betts, H.D., Trustrum, N.A., De Rose, R.C., 2003. Geomorphic changes in a complex gully system measured from sequential digital elevation models, and implications for management. Earth Surf. Process. Landf. 28, 1043–1058. https://doi.org/10.1002/esp.500.

Blair, N., Leu, A., Muñoz, E., Olsen, J., Kwong, E., Des Marais, D., 1985. Carbon isotopic fractionation in heterotrophic microbial metabolism. Appl. Environ. Microbiol. 50, 996–1001. https://doi.org/10.1128/aem.50.4.996-1001.1985.

Blattmann, T.M., Wang, S.-L., Lupker, M., Märki, L., Haghipour, N., Wacker, L., Chung, L.-H., Bernasconi, S.M., Plötze, M., Eglinton, T.I., 2019. Sulphuric acid-mediated weathering on Taiwan buffers geological atmospheric carbon sinks. Sci. Rep. 9, 2945. https://doi.org/10.1038/s41598-019-39272-5.

Bolton, E.W., Berner, R.A., Petsch, S.T., 2006. The Weathering of Sedimentary Organic Matter as a Control on Atmospheric O2: II. Theoretical modeling. Am. J. Sci. 306, 575–615. https://doi.org/10.2475/08.2006.01.

Bond-Lamberty, B., Thomson, A., 2010. A global database of soil respiration data. Biogeosciences 7, 1915–1926. https://doi.org/10.5194/bg-7-1915-2010.

Bosatta, E., Ågren, G.I., 1999. Soil organic matter quality interpreted thermodynamically. Soil Biol. Biochem. 31, 1889–1891. https://doi.org/10.1016/S0038-0717(99)00105-4.

Bouchez, J., Beyssac, O., Galy, V., Gaillardet, J., France-Lanord, C., Maurice, L., Moreira-Turcq, P., 2010. Oxidation of petrogenic organic carbon in the Amazon floodplain as a source of atmospheric CO2. Geology 38, 255–258. https://doi.org/10.1130/G30608.1.

Bufe, A., Hovius, N., Emberson, R., Rugenstein, J.K.C., Galy, A., Hassenruck-Gudipati, H. J., Chang, J., 2021. Co-variation of silicate, carbonate and sulfide weathering drives CO2 release with erosion. Nat. Geosci. 14, 211–216. https://doi.org/10.1038/s41561-021-00714-3.

Burke, A., Present, T.M., Paris, G., Rae, E.C.M., Sandilands, B.H., Gaillardet, J., Peucker-Ehrenbrink, B., Fischer, W.W., McClelland, J.W., Spencer, R.G.M., Voss, B.M., Adkins, J.F., 2018. Sulfur isotopes in rivers: Insights into global weathering budgets, pyrite oxidation, and the modern sulfur cycle. Earth Planet. Sci. Lett. 496, 168–177. https://doi.org/10.1016/j.epsl.2018.05.022.

Calmels, D., Gaillardet, J., Brenot, A., France-Lanord, C., 2007. Sustained sulfide oxidation by physical erosion processes in the Mackenzie River basin: climatic perspectives. Geology 35, 1003–1006. https://doi.org/10.1130/G24132A.1.

Calmels, D., Gaillardet, J., François, L., 2014. Sensitivity of carbonate weathering to soil CO2 production by biological activity along a temperate climate transect. Chem. Geol. 390, 74–86. https://doi.org/10.1016/j.chemgeo.2014.10.010.

Caves Rugenstein, J.K., Ibarra, D.E., von Blanckenburg, F., 2019. Neogene cooling driven by land surface reactivity rather than increased weathering fluxes. Nature 571, 99–102. https://doi.org/10.1038/s41586-019-1332-y.

Cerling, T.E., Barnette, J.E., Chesson, L.A., Douglas-Hamilton, I., Gobush, K.S., Uno, K.T., Wasser, S.K., Xu, X., 2016. Radiocarbon dating of seized ivory confirms rapid decline in African elephant populations and provides insight into illegal trade. Proc. Natl. Acad. Sci. 113, 13330–13335. https://doi.org/10.1073/pnas.1614938113.

Chamberlin, T.C., 1899. An attempt to Frame a working hypothesis of the cause of glacial periods on an atmospheric basis. J. Geol. 7, 545–584. https://doi.org/10.1086/608524.

Chang, S., Berner, R.A., 1999. Coal weathering and the geochemical carbon cycle. Geochim. Cosmochim. Acta 63, 3301–3310. https://doi.org/10.1016/S0016-7037(99)00252-5.

Chappell, P.R., 2016. The Climate and Weather of the Gisborne District. New Zealand, NIWA Science and Technology Series, p. 70.

Dalai, T.K., Singh, S.K., Trivedi, J.R., Krishnaswami, S., 2002. Dissolved rhenium in the Yamuna river system and the Ganga in the Himalaya: role of black shale weathering on the budgets of Re, Os, and U in rivers and CO2 in the atmosphere. Geochim. Cosmochim. Acta 66, 29–43. https://doi.org/10.1016/S0016-7037(01)00747-5.

Drever, J.I., 1994. The effect of land plants on weathering rates of silicate minerals. Geochim. Cosmochim. Acta 58, 2325–2332. https://doi.org/10.1016/0016-7037(94)90013-2.

Ebelmen, J.J., 1845. Sur les produits de la décomposition des espèces minérales de la famille des silicates. Ann. Min. 7, 3–66.

Ehrlich, H.L., Newman, D.K., Kappler, A., 2015. Ehrlich's Geomicrobiology, 6th ed. CRC Press, Boca Raton, USA. https://doi.org/10.1201/b19121.

Erba, E., 2004. Calcareous nannofossils and Mesozoic oceanic anoxic events. Mar. Micropaleontol. 52, 85–106. https://doi.org/10.1016/j.marmicro.2004.04.007.

Etiope, G., Klusman, R.W., 2002. Geologic emissions of methane to the atmosphere. Chemosphere 49, 777–789. https://doi.org/10.1016/S0045-6535(02)00380-6.

Etiope, G., Klusman, R.W., 2010. Microseepage in drylands: flux and implications in the global atmospheric source/sink budget of methane. Glob. Planet. Chang. 72, 265–274. https://doi.org/10.1016/j.gloplacha.2010.01.002.

Evans, M.J., Derry, L.A., France-Lanord, C., 2008. Degassing of metamorphic carbon dioxide from the Nepal Himalaya. Geochem. Geophys. Geosyst. 9, Q04021. https://doi.org/10.1029/2007GC001796.

Feng, G., Wu, L., Letey, J., 2002. Evaluating aeration criteria by simultaneous measurement of oxygen diffusion rate and soil-water regime. Soil Sci. 167, 495–503. https://doi.org/10.1097/00010694-200208000-00001.

Francis, D.A., Christie, A.B., Brown, L.J., 1991. Sheet QM 303, Raukumara: geological resource map of New Zealand, 1:250 000. In: New Zealand Geological Survey Report M180.

Gaillardet, J., Dupré, B., Louvat, P., Allègre, C.J., 1999. Global silicate weathering and CO2 consumption rates deduced from the chemistry of large rivers. Chem. Geol. 159, 3–30. https://doi.org/10.1016/S0009-2541(99)00031-5.

Galy, V., Peucker-Ehrenbrink, B., Eglinton, T., 2015. Global carbon export from the terrestrial biosphere controlled by erosion. Nature 521, 204–207. https://doi.org/10.1038/nature14400.

Garnett, M.H., Murray, C., 2013. Processing of CO2 samples collected using zeolite molecular Sieve for 14C analysis at the NERC radiocarbon facility (East Kilbride, UK). Radiocarbon 55, 410–415. https://doi.org/10.1017/S0033822200057532.

Garnett, M.H., Newton, J.-A., Ascough, P.L., 2019. Advances in the radiocarbon analysis of carbon dioxide at the NERC radiocarbon facility (East Kilbride) using molecular sieve cartridges. Radiocarbon 61, 1855–1865. https://doi.org/10.1017/RDC.2019.86.

Giggenbach, W.F., 1997. Relative importance of thermodynamic and kinetic processes in governing the chemical and isotopic composition of carbon gases in high-heatflow sedimentary basins. Geochim. Cosmochim. Acta 61, 3763–3785. https://doi.org/10.1016/S0016-7037(97)00171-3.

Giggenbach, W.F., Sano, Y., Wakita, H., 1993. Isotopic composition of helium, and CO2 and CH4 contents in gases produced along the New Zealand part of a convergent plate boundary. Geochim. Cosmochim. Acta 57, 3427–3455. https://doi.org/10.1016/0016-7037(93)90549-C.

Giggenbach, W.F., Stewart, M.K., Sano, Y., Goguel, R.L., Lyon, G.L., 1995. Isotopic and chemical composition of waters and gases from the East Coast Accretionary Prism, New Zealand. Int. Atom. Energy Agency Conf. Proc. 788, 209–231.

Gomez, B., Brackley, H.L., Hicks, D.M., Neff, H., Rogers, K.M., 2004. Organic carbon in floodplain alluvium: signature of historic variations in erosion processes associated with deforestation, Waipaoa River basin, New Zealand. J. Geophys. Res. 109, F04011. https://doi.org/10.1029/2004JF000154.

Gröcke, D.R., Price, G.D., Ruffell, A.H., Mutterlose, J., Baraboshkin, E., 2003. Isotopic evidence for Late Jurassic–Early Cretaceous climate change. Palaeogeogr. Palaeoclimatol. Palaeoecol. 202, 97–118. https://doi.org/10.1016/S0031-0182(03)00631-X.

Gu, X., Rempe, D.M., Dietrich, W.E., West, A.J., Lin, T.-C., Jin, L., Brantley, S.L., 2020. Chemical reactions, porosity, and microfracturing in shale during weathering: the effect of erosion rate. Geochim. Cosmochim. Acta 269, 63–100. https://doi.org/10.1016/j.gca.2019.09.044.

Hardie, S.M.L., Garnett, M.H., Fallick, A.E., Rowland, A.P., Ostle, N.J., 2005. Carbon dioxide capture using a zeolite molecular sieve sampling system for isotopic studies (13C and 14C) of respiration. Radiocarbon 47, 441–451. https://doi.org/10.1017/S0033822200035220.

Hasenmueller, E.A., Jin, L., Stinchcomb, G.E., Lin, H., Brantley, S.L., Kaye, J.P., 2015. Topographic controls on the depth distribution of soil CO2 in a small temperate watershed. Appl. Geochem. 63, 58–69. https://doi.org/10.1016/j.apgeochem.2015.07.005.

Hemingway, J.D., Rothman, D.H., Rosengard, S.Z., Galy, V.V., 2017. Technical note: an inverse method to relate organic carbon reactivity to isotope composition from serial oxidation. Biogeosciences 14, 5099–5114. https://doi.org/10.5194/bg-14-5099-2017.

Hemingway, J.D., Hilton, R.G., Hovius, N., Eglinton, T.I., Haghipour, N., Wacker, L., Chen, M.-C., Galy, V.V., 2018. Microbial oxidation of lithospheric organic carbon in rapidly eroding tropical mountain soils. Science 360, 209–212. https://doi.org/10.1126/science.aao6463.

Hemingway, J.D., Rothman, D.H., Grant, K.E., Rosengard, S.Z., Eglinton, T.I., Derry, L.A., Galy, V.V., 2019. Mineral protection regulates long-term global preservation of natural organic carbon. Nature 570, 228–231. https://doi.org/10.1038/s41586-019-1280-6.

Hicks, D.M., Gomez, B., Trustrum, N.A., 2000. Erosion thresholds and suspended sediment yields, Waipaoa River Basin, New Zealand. Water Resour. Res. 36, 1129–1142. https://doi.org/10.1029/1999WR900340.

Hicks, D.M., Gomez, B., Trustrum, N.A., 2004. Event Suspended sediment characteristics and the generation of hyperpycnal plumes at river mouths: east coast continental margin, North Island, New Zealand. J. Geol. 112, 471–485. https://doi.org/10.1086/421075.

Hilton, R.G., 2017. Climate regulates the erosional carbon export from the terrestrial biosphere. Geomorphology 277, 118–132. https://doi.org/10.1016/j.geomorph.2016.03.028.

Hilton, R.G., West, A.J., 2020. Mountains, erosion and the carbon cycle. Nat. Rev. Earth Environ. 1, 284–299. https://doi.org/10.1038/s43017-020-0058-6.

Hilton, R.G., Galy, A., Hovius, N., Horng, M.-J., Chen, H., 2011. Efficient transport of fossil organic carbon to the ocean by steep mountain rivers: an orogenic carbon sequestration mechanism. Geology 39, 71–74. https://doi.org/10.1130/G31352.1.

Hilton, R.G., Gaillardet, J., Calmels, D., Birck, J.-L., 2014. Geological respiration of a mountain belt revealed by the trace element rhenium. Earth Planet. Sci. Lett. 403, 27–36. https://doi.org/10.1016/j.epsl.2014.06.021.

Hoefs, J., Frey, M., 1976. The isotopic composition of carbonaceous matter in a metamorphic profile from the Swiss Alps. Geochim. Cosmochim. Acta 40, 945–951. https://doi.org/10.1016/0016-7037(76)90143-5.

Hopmans, J.W., Šimunek, J., Bristow, K.L., 2002. Indirect estimation of soil thermal properties and water flux using heat pulse probe measurements: Geometry and dispersion effects. Water Resour. Res. 38, 1006. https://doi.org/10.1029/2000WR000071.

Hua, Q., Barbetti, M., Rakowski, A.Z., 2013. Atmospheric Radiocarbon for the period 1950–2010. Radiocarbon 55, 2059–2072. https://doi.org/10.2458/azu_js_rc.v55i2.16177.

Isson, T.T., Planavsky, N.J., Coogan, L.A., Stewart, E.M., Ague, J.J., Bolton, E.W., Zhang, S., McKenzie, N.R., Kump, L.R., 2020. Evolution of the Global Carbon Cycle and climate Regulation on Earth. Glob. Biogeochem. Cycles 34. https://doi.org/10.1029/2018GB006061 e2018GB006061.

Jin, L., Ogrinc, N., Yesavage, T., Hasenmueller, E.A., Ma, L., Sullivan, P.L., Kaye, J., Duffy, C., Brantley, S.L., 2014. The CO2 consumption potential during gray shale weathering: Insights from the evolution of carbon isotopes in the Susquehanna Shale Hills critical zone observatory. Geochim. Cosmochim. Acta 142, 260–280. https://doi.org/10.1016/j.gca.2014.07.006.

Keller, C.K., Bacon, D.H., 1998. Soil respiration and georespiration distinguished by transport analyses of vadose CO2, 13CO2, and 14CO2. Glob. Biogeochem. Cycles 12, 361–372. https://doi.org/10.1029/98GB00742.

Kenny, J.A., 1984. Petrography of cretaceous and Tertiary sedimentary rocks of the Ihungia catchment, Raukumara Peninsula, North Island, New Zealand. N. Z. J. Geol. Geophys. 27, 291–298.

Larsen, I.J., Montgomery, D.R., Greenberg, H.M., 2014. The contribution of mountains to global denudation. Geology 42, 527–530. https://doi.org/10.1130/G35136.1.

Leifeld, J., von Lützow, M., 2014. Chemical and microbial activation energies of soil organic matter decomposition. Biol. Fertil. Soils 50, 147–153. https://doi.org/10.1007/s00374-013-0822-6.

Leithold, E.L., Blair, N.E., Perkey, D.W., 2006. Geomorphologic controls on the age of particulate organic carbon from small mountainous and upland rivers. Glob. Biogeochem. Cycles 20, GB3022. https://doi.org/10.1029/2005GB002677.

Li, S.-L., Calmels, D., Han, G., Gaillardet, J., Liu, C.-Q., 2008. Sulfuric acid as an agent of carbonate weathering constrained by δ13CDIC: examples from Southwest China. Earth Planet. Sci. Lett. 270, 189–199. https://doi.org/10.1016/j.epsl.2008.02.039.

Litchfield, N., Berryman, K., 2006. Relations between postglacial fluvial incision rates and uplift rates in the North Island, New Zealand. J. Geophys. Res. 111, F02007. https://doi.org/10.1029/2005JF000374.

Longbottom, T.L., Hockaday, W.C., 2019. Molecular and isotopic composition of modern soils derived from kerogen-rich bedrock and implications for the global C cycle. Biogeochemistry 143, 239–255. https://doi.org/10.1007/s10533-019-00559-4.
Lowry, D.C., Francis, D.A., Bennett, D.J., 1998. Biogenic gas: a new play in the East Coast Basin of New Zealand. In: New Zealand Petroleum Conference, pp. 207–221.
Lu, N., Godt, J., 2013. Hillslope Hydrology and Stability. Cambridge University Press, Cambridge, UK. https://doi.org/10.1017/CBO9781139108164.
Lyon, G.L., Giggenbach, W.F., 1992. The stable isotope composition of some East Coast natural gases. In: New Zealand Petroleum Conference, pp. 310–319.
Lyons, W.B., Carey, A.E., Hicks, D.M., Nezat, C.A., 2005. Chemical weathering in high-sediment-yielding watersheds, New Zealand. J. Geophys. Res. 110, F01008. https://doi.org/10.1029/2003JF000088.
Maher, K., Chamberlain, C.P., 2014. Hydrologic regulation of chemical weathering and the geologic carbon cycle. Science 343, 1502–1504. https://doi.org/10.1126/science.1250770.
Marden, M., Arnold, G., Seymour, A., Hambling, R., 2012. History and distribution of steepland gullies in response to land use change, East Coast Region, North Island, New Zealand. Geomorphology 153–154, 81–90. https://doi.org/10.1016/j.geomorph.2012.02.011.
Mason, D.C., Garcia-Pintado, J., Cloke, H.L., Dance, S.L., 2016. Evidence of a topographic signal in surface soil moisture derived from ENVISAT ASAR wide swath data. Int. J. Appl. Earth Obs. Geoinf. 45, 178–186. https://doi.org/10.1016/j.jag.2015.02.004.
Mathys, N., Brochot, S., Meunier, M., Richard, D., 2003. Erosion quantification in the small marly experimental catchments of Draix (Alpes de Haute Provence, France). Calibration of the ETC rainfall–runoff–erosion model. Catena (Amst) 50, 527–548. https://doi.org/10.1016/S0341-8162(02)00122-4.
Matlakowska, R., Sklodowska, A., 2011. Biodegradation of Kupferschiefer black shale organic matter (Fore-Sudetic Monocline, Poland) by indigenous microorganisms. Chemosphere 83, 1255–1261. https://doi.org/10.1016/j.chemosphere.2011.03.003.
Mazengarb, C., Speden, I.G., 2000. Geological Map of the Raukumara Area [Map], 6th ed. Institute of Geological & Nuclear Sciences, Lower Hutt, New Zealand https://www.gns.cri.nz/Home/Our-Science/Land-and-Marine-Geoscience/Regional-Geology/Geological-Maps/1-250-000-Geological-Map-of-New-Zealand-QMAP/QMAP-text-maps#raukumara.
Menzies, C.D., Wright, S.L., Craw, D., James, R.H., Alt, J.C., Cox, S.C., Pitcairn, I.K., Teagle, D.A.H., 2018. Carbon dioxide generation and drawdown during active orogenesis of siliciclastic rocks in the Southern Alps, New Zealand. Earth Planet. Sci. Lett. 481, 305–315. https://doi.org/10.1016/j.epsl.2017.10.010.
Milliman, J.D., Syvitski, J.P.M., 1992. Geomorphic/tectonic control of sediment discharge to the Ocean: the importance of small mountainous rivers. The Journal of Geology 100, 525–544. https://doi.org/10.1086/629606.
Moon, S., Chamberlain, C.P., Hilley, G.E., 2014. New estimates of silicate weathering rates and their uncertainties in global rivers. Geochim. Cosmochim. Acta 134, 257–274. https://doi.org/10.1016/j.gca.2014.02.033.
Nelson, C.S., Smith, A.M., 1996. Stable oxygen and carbon isotope compositional fields for skeletal and diagenetic components in New Zealand Cenozoic nontropical carbonate sediments and limestones: a synthesis and review. N. Z. J. Geol. Geophys. 39, 93–107. https://doi.org/10.1080/00288306.1996.9514697.
Neu, V., Ward, N.D., Krusche, A.V., Neill, C., 2016. Dissolved organic and inorganic carbon flow paths in an Amazonian transitional forest. Front. Mar. Sci. 3, 114. https://doi.org/10.3389/fmars.2016.00114.
Oertel, C., Matschullat, J., Zurba, K., Zimmermann, F., Erasmi, S., 2016. Greenhouse gas emissions from soils—a review. Geochemistry 76, 327–352. https://doi.org/10.1016/j.chemer.2016.04.002.
Parkner, T., Page, M.J., Marutani, T., Trustrum, N.A., 2006. Development and controlling factors of gullies and gully complexes, East Coast, New Zealand. Earth Surf. Process. Landf. 31, 187–199. https://doi.org/10.1002/esp.1321.
Pearson, M.J., Nelson, C.S., 2005. Organic geochemistry and stable isotope composition of New Zealand carbonate concretions and calcite fracture fills. N. Z. J. Geol. Geophys. 48, 395–414. https://doi.org/10.1080/00288306.2005.9515122.
Petsch, S.T., 2014. Weathering of organic carbon. In: Treatise on Geochemistry. Elsevier, Amsterdam, Netherlands, pp. 217–238. https://doi.org/10.1016/B978-0-08-095975-7.01013-5.
Petsch, S.T., Eglinton, T.I., Edwards, K.J., 2001. 14C-dead living biomass: evidence for microbial assimilation of ancient organic carbon during shale weathering. Science 292, 1127–1131. https://doi.org/10.1126/science.1058332.
Pirk, N., Mastepanov, M., Parmentier, F.-J.W., Lund, M., Crill, P., Christensen, T.R., 2016. Calculations of automatic chamber flux measurements of methane and carbon dioxide using short time series of concentrations. Biogeosciences 13, 903–912. https://doi.org/10.5194/bg-13-903-2016.
Raich, J.W., Schlesinger, W.H., 1992. The global carbon dioxide flux in soil respiration and its relationship to vegetation and climate. Tellus 44B, 81–99. https://doi.org/10.1034/j.1600-0889.1992.t01-1-00001.x.
Raymond, P.A., Hartmann, J., Lauerwald, R., Sobek, S., McDonald, C., Hoover, M., Butman, D., Striegl, R., Mayorga, E., Humborg, C., Kortelainen, P., Dürr, H., Meybeck, M., Ciais, P., Guth, P., 2013. Global carbon dioxide emissions from inland waters. Nature 503, 355–359. https://doi.org/10.1038/nature12760.
Reimer, P.J., Brown, T.A., Reimer, R.W., 2004. Discussion: reporting and calibration of post-bomb 14 C data. Radiocarbon 46, 1299–1304. https://doi.org/10.1017/S0033822200033154.
Reyes, A.G., Christenson, B.W., Faure, K., 2010. Sources of solutes and heat in low-enthalpy mineral waters and their relation to tectonic setting, New Zealand. J. Volcanol. Geotherm. Res. 192, 117–141. https://doi.org/10.1016/j.jvolgeores.2010.02.015.
Romio, L.C., Roberti, D.R., Buligon, L., Zimmer, T., Degrazia, G.A., 2019. A numerical model to estimate the soil thermal conductivity using field experimental data. Appl. Sci. 9, 4799. https://doi.org/10.3390/app9224799.
Šantrůčková, H., Bird, M.I., Lloyd, J., 2000. Microbial processes and carbon-isotope fractionation in tropical and temperate grassland soils. Funct. Ecol. 14, 108–114. https://doi.org/10.1046/j.1365-2435.2000.00402.x.
Scadden, P., Dooley, D., Boyes, A., 2016. Petroleum Basin Explorer [Data Set], 3.3.3. ed. Institute of Geological & Nuclear Sciences, Lower Hutt, New Zealand https://www.gns.cri.nz/Home/Our-Science/Energy-Futures/Oil-and-Gas/Petroleum-Basin-Explorer.
Schillawski, S., Petsch, S., 2008. Release of biodegradable dissolved organic matter from ancient sedimentary rocks. Glob. Biogeochem. Cycles 22, GB3002. https://doi.org/10.1029/2007GB002980.
Schmidt, M.W.I., Torn, M.S., Abiven, S., Dittmar, T., Guggenberger, G., Janssens, I.A., Kleber, M., Kögel-Knabner, I., Lehmann, J., Manning, D.A.C., Nannipieri, P., Rasse, D.P., Weiner, S., Trumbore, S.E., 2011. Persistence of soil organic matter as an ecosystem property. Nature 478, 49–56. https://doi.org/10.1038/nature10386.
Schwab, V.F., Nowak, M.E., Elder, C.D., Trumbore, S.E., Xu, X., Gleixner, G., Lehmann, R., Pohnert, G., Muhr, J., Küsel, K., Totsche, K.U., 2019. 14C-free carbon is a major contributor to cellular biomass in geochemically distinct groundwater of shallow sedimentary Bedrock aquifers. Water Resour. Res. 55, 2104–2121. https://doi.org/10.1029/2017WR022067.
Seifert, A.-G., Trumbore, S., Xu, X., Zhang, D., Kothe, E., Gleixner, G., 2011. Variable effects of labile carbon on the carbon use of different microbial groups in black slate degradation. Geochim. Cosmochim. Acta 75, 2557–2570. https://doi.org/10.1016/j.gca.2011.02.037.
Seifert, A.-G., Trumbore, S., Xu, X., Zhang, D., Gleixner, G., 2013. Variable effects of plant colonization on black slate uptake into microbial PLFAs. Geochim. Cosmochim. Acta 106, 391–403. https://doi.org/10.1016/j.gca.2012.12.011.
Shulmeister, J., 2017. Landscape and Quaternary Environmental Change in New Zealand. Atlantis Press, Paris, France. https://doi.org/10.2991/978-94-6239-237-3.
Soulet, G., Hilton, R.G., Garnett, M.H., Dellinger, M., Croissant, T., Ogrič, M., Klotz, S., 2018. Technical note: in situ measurement of flux and isotopic composition of CO2 released during oxidative weathering of sedimentary rocks. Biogeosciences 15, 4087–4102. https://doi.org/10.5194/bg-15-4087-2018.
Soulet, G., Hilton, R.G., Garnett, M.H., Roylands, T., Klotz, S., Croissant, T., Dellinger, M., Le Bouteiller, C., 2021. Temperature control on CO2 emissions from the weathering of sedimentary rocks. Nat. Geosci. 14, 665–671. https://doi.org/10.1038/s41561-021-00805-1.
Speden, I.G., 1976. Geology of Mt Taitai, Tapuaeroa valley, Raukumara Peninsula. N. Z. J. Geol. Geophys. 19, 71–119.
Stasiuk, R., Włodarczyk, A., Karcz, P., Janas, M., Skłodowska, A., Matlakowska, R., 2017. Bacterial weathering of fossil organic matter and organic carbon mobilization from subterrestrial Kupferschiefer black shale: long-term laboratory studies. Environ. Microbiol. Rep. 9, 459–466. https://doi.org/10.1111/1758-2229.12559.
Stuiver, M., Polach, H.A., 1977. Discussion reporting of 14C data. Radiocarbon 19, 355–363. https://doi.org/10.1017/S0033822200003672.
Sundquist, E.T., Visser, K., 2003. The geologic history of the carbon cycle. In: Treatise on Geochemistry. Elsevier, Amsterdam, Netherlands, pp. 425–472. https://doi.org/10.1016/B0-08-043751-6/08133-0.
Thompson, C.E., 2009. Tracking Organic Matter from Source to Sink in the Waiapu River Watershed, New Zealand: A Geochemical Perspective. Doctoral thesis. NC State University, Raleigh, USA.
Torres, M.A., West, A.J., Li, G., 2014. Sulphide oxidation and carbonate dissolution as a source of CO2 over geological timescales. Nature 507, 346–349. https://doi.org/10.1038/nature13030.
Tremosa, J., Debure, M., Narayanasamy, S., Redon, P.-O., Jacques, D., Claret, F., Robinet, J.-C., 2020. Shale weathering: a lysimeter and modelling study for flow, transport, gas diffusion and reactivity assessment in the critical zone. J. Hydrol. 587, 124925 https://doi.org/10.1016/j.jhydrol.2020.124925.
Tune, A.K., Druhan, J.L., Wang, J., Bennett, P.C., Rempe, D.M., 2020. Carbon dioxide production in Bedrock beneath soils substantially contributes to forest carbon cycling. J. Geophys. Res. Biogeosci. 125 https://doi.org/10.1029/2020JG005795 e2020JG005795.
Turnbull, J.C., Mikaloff Fletcher, S.E., Ansell, I., Brailsford, G.W., Moss, R.C., Norris, M. W., Steinkamp, K., 2017. Sixty years of radiocarbon dioxide measurements at Wellington, New Zealand: 1954–2014. Atmos. Chem. Phys. 17, 14771–14784. https://doi.org/10.5194/acp-17-14771-2017.
Voroney, R.P., Heck, R.J., 2015. The soil habitat. In: Paul, E.A. (Ed.), Soil Microbiology, Ecology and Biochemistry. Academic Press, London, UK, pp. 15–39. https://doi.org/10.1016/C2011-0-05497-2.
Waksman, S.A., Starkey, R.L., 1931. The Soil and the Microbe. J. Wiley & Sons, Inc., New York, USA https://doi.org/10.5962/bhl.title.7227.
Walker, J.C.G., Hays, P.B., Kasting, J.F., 1981. A negative feedback mechanism for the long-term stabilization of Earth's surface temperature. J. Geophys. Res. 86, 9776. https://doi.org/10.1029/JC086iC10p09776.
Weissert, H., Lini, A., Föllmi, K.B., Kuhn, O., 1998. Correlation of Early Cretaceous carbon isotope stratigraphy and platform drowning events: a possible link? Palaeogeogr. Palaeoclimatol. Palaeoecol. 137, 189–203. https://doi.org/10.1016/S0031-0182(97)00109-0.
Werth, M., Kuzyakov, Y., 2010. 13C fractionation at the root–microorganisms–soil interface: a review and outlook for partitioning studies. Soil Biol. Biochem. 42, 1372–1384. https://doi.org/10.1016/j.soilbio.2010.04.009.

West, A.J., Galy, A., Bickle, M., 2005. Tectonic and climatic controls on silicate weathering. Earth Planet. Sci. Lett. 235, 211–228. https://doi.org/10.1016/j.epsl.2005.03.020.

Whiticar, M.J., 1999. Carbon and hydrogen isotope systematics of bacterial formation and oxidation of methane. Chem. Geol. 161, 291–314. https://doi.org/10.1016/S0009-2541(99)00092-3.

Włodarczyk, A., Lirski, M., Fogtman, A., Koblowska, M., Bidziński, G., Matlakowska, R., 2018. The oxidative metabolism of fossil hydrocarbons and sulfide minerals by the lithobiontic microbial community inhabiting deep subterrestrial Kupferschiefer Black Shale. Front. Microbiol. 9, 972. https://doi.org/10.3389/fmicb.2018.00972.